

MD97

## D3.2 Overview report of digital twins

Synergetics | Synergies for Green Transformation of Inland and Coastal Shipping

<b>GRANT AGREEMENT NO.</b>	101096809
<b>DURATION OF THE PROJECT</b>	42 months
<b>DELIVERABLE NUMBER</b>	D3.2
<b>DISSEMINATION LEVEL</b>	PU
<b>DELIVERABLE LEADER</b>	MARIN
<b>STATUS</b>	FINAL
<b>SUBMISSION DATE</b>	17-06-2026
<b>AUTHOR</b>	P. Garcia Barrena, MARIN p.garcia@marin.nl
<b>CO-AUTHOR</b>	Alessandro Gubbini MARIN a.gubbini@marin.nl

Co-Funded by the European Union. Views and opinions expressed are however those of the authors only and do not necessarily reflect those of the European Union or CINEA. Neither the European Union nor the granting authority can be held responsible for them.



## | Table of Content

1.	Introduction .....	12
2.	Overview of the concept design .....	13
2.1	Operational Analysis overview .....	14
2.2	Propulsion, power and energy concept design .....	16
2.3	Test cases definition .....	17
2.3.1	Quasi-static test cases .....	18
2.3.1.1	Test case TC-1: Quasi Static simulation of the reference design based on the "Maintenance of the Danube" operation .....	19
2.3.1.2	Test case TC-2: Quasi Static simulation of the new design based on the "Maintenance of the Danube" operation .....	19
2.3.2	Dynamic test cases .....	20
2.3.2.1	Test case TC-4: Stopping capacity .....	20
2.3.2.2	Test case TC-5: Capacity for taking evasive action .....	21
2.3.2.3	Test case TC-6: Turning capacity .....	22
3.	Propulsion, Power and Energy system modelling .....	24
3.1	Virtual model of the power systems for quasi-static simulations .....	24
3.1.1	Fuel consumption maps .....	26
3.1.2	Emissions calculation .....	27
3.2	Virtual model of the new power system for dynamic simulations .....	28
3.2.1	AC Distribution System .....	29
3.2.2	Genset Models .....	29
3.2.2.1	Internal Combustion Engine (ICE) Models .....	29
3.2.2.2	Alternator Model .....	30
3.2.2.3	Gensets control logic - Droop Control .....	31
3.2.3	Propulsion motors .....	34
3.2.4	Hydrodynamic model .....	34
3.2.4.1	Coordinate system .....	35
3.2.4.2	Hydrostatics .....	35
3.2.4.3	Resistance .....	36
3.2.4.4	Manoeuvring reaction forces .....	36
3.2.4.5	Propeller and duct open water characteristics .....	36
3.2.4.6	Wind forces and moments .....	38
3.2.4.7	Rudder .....	39
3.3	Control and Automation .....	39
3.3.1	Power Management System (PMS) .....	39



3.3.1.1	Operational Mode .....	39
3.3.1.2	Control Calculation Chain .....	40
3.3.2	Propulsion Management System.....	41
4.	Results of verification tests.....	43
4.1	Results of quasi-static test cases .....	43
4.2	Results of dynamic test cases .....	47
4.2.1	Test case TC-4: Stopping capacity.....	47
4.2.2	Test case TC-5: Capacity for taking evasive action .....	49
4.2.3	Test case TC-6: Turning capacity .....	51
5.	Conclusions .....	53
6.	Bibliography .....	54



## | List of Figures

Figure 1-1: Schematic representation of the W-model for product design.....	12
Figure 2-1: BIO II (Maintenance of the Danube River) power time profile .....	15
Figure 2-2: Single line diagram of the new propulsion, power and energy systems .....	16
Figure 2-3: Overview of the power losses for the reference diesel direct (left) and new methanol electric (right) system architecture.....	18
Figure 2-4: Diesel direct quasi static model calculation chain. ....	19
Figure 2-5: Genset electric quasi static model calculation chain. ....	19
Figure 2-6: Example of diagram of the distance covered and speed of vessel during the stopping manoeuvre. ....	20
Figure 2-7: Diagram of the evasive action manoeuvre described in instruction ESI-II-4 of ES-TRIN. ..	22
Figure 2-8: Schematic representation of the test sequence to be followed in test case TC-5 (left) and TC-6 (right). Barge has not been included in the drawing.....	23
Figure 3-1: Simulink Model used for the quasi-static simulations.....	24
Figure 3-2: Quasi-static test model. ....	25
Figure 3-3: Fuel consumption maps. ....	26
Figure 3-4: Comparison of the main components of the single line diagram (right) with those of the dynamic model (left) of the new power and energy system of the push boat, used for the dynamic test cases.....	28
Figure 3-5: Power curves for the modelled 175 kW (left) and 410 kW (right) single fuel MD97 engines. ....	29
Figure 3-6: Droop lines of the methanol gensets used for load sharing the dynamic simulation. ....	31
Figure 3-7: Example of genset synchronization procedure. ....	32
Figure 3-8: Overview of the v-ZEL dynamic model used for the methanol gensets. ....	33
Figure 3-9: Characteristic curves (blue = torque; orange = power) used for the dynamic model of the electric motors used for propulsion. ....	34
Figure 3-10: Ship-fixed coordinate system used for the simulations for the dynamic test cases. ....	35
Figure 3-11: Thrust coefficient (CT) as function of the angle of advance ( $\beta$ ) and the inflow angle ( $\theta$ , $\pm 20$ , $\pm 40$ and $\pm 90$ degrees).....	37
Figure 3-12: Torque coefficient (CQ) as function of the angle of advance ( $\beta$ ) and the inflow angle ( $\theta$ , $\pm 20$ , $\pm 40$ and $\pm 90$ degrees).....	38
Figure 3-13: Wind coefficients used for the calculation of the wind force in longitudinal (Cx) and transverse direction (Cy), and the yaw wind moment (Cn). ....	39
Figure 3-14: PMS Control Strategy Diagram. ....	41
Figure 3-15: Characteristic curves (blue = torque; orange = power) of the electric motors used for propulsion, indicating some parameters used for the propulsion management system.....	42
Figure 4-1: Cumulative fuel mass (left) and volume (right) consumed during the operation 'Maintenance of the Danube' (BIO II) for the current (blue) and new (orange) power and energy system architecture of Demo 6. ....	43



Figure 4-2: Well-to-wake emissions for the current (diesel/HVO) and the new design (bio-Methanol) when performing the operations defined by BIO II. ....45

Figure 4-3: Relative reduction in well-to-wake emissions for the current design running with HVO and the new design using bio-Methanol, with respect to the current design running on diesel.....46

Figure 4-4: Distance covered and speed of vessel in relation to the ground during the stopping manoeuvre simulation performed in test case TC-4. The letters describe the most important points of the manoeuvre as defined in section 2.3.2.1.....48

Figure 4-5: Time series of the rudder angle and turning rate resulting from the simulations of test case TC-5 for the evasive manoeuvre at 20 degrees rudder angle. ....50

Figure 4-6: Time series of the rudder angle and turning rate resulting from the simulations of test case TC-5 for the evasive manoeuvre at 45 degrees rudder angle. ....51

Figure 4-7: Top view showing the trajectory of the ship and barge and the relevant output parameters for test case TC6. ....52



## | List of Tables

Table 1-1: Release Approval.....	7
Table 2-1: Main particulars of the Bad Deutsch Altenburg. ....	13
Table 2-2: Overview of the operational analysis.....	14
Table 2-3: Assumed components efficiency. ....	18
Table 2-4: Limit values allowed for the evasive manoeuvre performed in test case TC5. ....	21
Table 3-1 Simulation settings used for the quasi-static test model. ....	25
Table 3-2: Lower Heating Value (LHV) of the fuels used in the simulations. ....	27
Table 3-3: CO <sub>2</sub> equivalent emission factors used for the emission calculations. ....	27
Table 3-4: NO <sub>x</sub> and PM emission factors used for the emission calculations. ....	28
Table 3-5: Overview of the conditions that define the open water characteristics for four quadrants..	36
Table 4-1: Overview of the fuel and energy consumed for the test cases 1 and 2. ....	43
Table 4-2: Overview of the emissions of the current and new design resulting from the quasi-static test cases TC-1 and TC-2. ....	44
Table 4-3: Main parameters for the stopping capacity of the new barge evaluated in test case TC4. ...	47
Table 4-4: Results of the simulations of evasive action manoeuvres performed for test case TC-5. ....	49
Table 4-5: Output parameters from the turning circle manoeuvre conducted for test case TC6.....	51



## | Release Approval

Table 1-1: Release Approval

Name	Role
V. Klisarić (CRS)	Reviewer 1
B. Friedhoff (DST)	Reviewer 2
B. Friedhoff (DST)	Coordinator



## | Abbreviations

AC	Alternating current
BIO	Bunker Independent Operation
CI	Compression Ignited
CO <sub>2</sub> eq	Carbon Dioxide equivalent emissions
EPM	Electric propulsion motor
ESM	Electric Shaft Machine (i.e., electric motor)
GHG	Green House Gas
GWP	Global Warming Potential
HVO	Hydrotreated Vegetable Oil
ICE	Internal Combustion Engine
LHV	Lower Heating Value
MCR	Maximum Continuous Rating
MeOH	Methanol
PMS	Power Management System
SF	Single Fuel
SOG	Speed Over Ground
TTW	Tank-to-Wake
WTT	Well-to-Tank
WTW	Well-to-Wake



## | List of symbols

<b>Symbol</b>	<b>Unit</b>	<b>Definition</b>
AD	m	Advance (turning capacity)
$A_x$	m <sup>2</sup>	Frontal area of the ship exposed to wind
$A_y$	m <sup>2</sup>	Side area of the ship exposed to wind
$C_n$	-	Coefficient for the yaw moment
$C_Q$	-	Torque coefficient
$C_T$	-	Thrust coefficient
$C_x$	-	Coefficient for the wind force in forward direction
$C_y$	-	Coefficient for the wind force in transverse direction
D	m	Propeller diameter
Dc	M	Turning circle diameter
D <sub>IST</sub>	m <sup>3</sup>	Loading condition (stopping capacity manoeuvre)
$GM_l$	m	Longitudinal metacentric height
$GM_t$	m	Transverse metacentric height
$J_{eq}$	kg·m <sup>2</sup>	Equivalent moment of inertia
$K_g$	kg·s <sup>-2</sup>	Stiffness matrix
$L_{oa}$	m	Length over all
$N_p$	-	Number of poles of the generator
n	s <sup>-1</sup>	Propeller rotation rate
$n_{ICE}$	rpm	Rotational speed of the ICE
$P_{el}$	W	Total electrical power requested by the power consumers
$P_{ICE}$	W	Mechanical power delivered by ICE
r	deg·min	Turning rate
SMESSUNG	m	Stopping distance in relation to the water (stopping capacity manoeuvre)
SL	m	Stopping distance in relation to the ground (stopping capacity manoeuvre)
$T_{ICE}$	N·m	Torque generated by ICE
T <sub>IST</sub>	m	Actual draught of convoy (stopping capacity manoeuvre)
$T_r$	N·m	Resistive torque
TD	m	Tactical diameter (turning capacity)
TR	m	Transfer (turning capacity)
U	m·s <sup>-1</sup>	Apparent wind speed



<b><u>Symbol</u></b>	<b><u>Unit</u></b>	<b><u>Definition</u></b>
$V_a$	$m \cdot s^{-1}$	Advance velocity
$V_{STR}$	$km \cdot h^{-1}$	Current velocity (stopping capacity manoeuvre)
$V_S$	$km \cdot h^{-1}$	Speed velocity (stopping capacity manoeuvre)
$b$	deg	Drift angle or Propeller angle of advance
$\delta$	deg	Rudder angle
$\eta_{Gen}$	-	Generator system efficiency
$\rho$	$kg \cdot m^{-3}$	Density of water
$\rho_a$	$kg \cdot m^{-3}$	Density of air
$\omega_{ICE}$	$s^{-1}$	Rotational speed of ICE
$\dot{\omega}_{ICE}$	$s^{-2}$	Rotational acceleration of ICE



## | Executive Summary

This report provides an overview on the virtual simulations that are part of Subtask 3.1.2 of Work Package 3 of Innovation Action SYNERGETICS. The objective of the virtual simulations carried out in this Subtask and reported in this deliverable are to conduct a performance analysis of the new design of Demonstrator 6 (push boat for Austrian waterway operator and SYNERGETICS partner viadonau). The new design consists of a methanol-electric propulsion system using methanol compression-ignited single-fuel gensets for power generation. This performance analysis is carried out by evaluating the compliance of the propulsion, power and energy system of the new design with the design requirements established during the operational analysis and conceptual design conducted in deliverables D3.1 [1] and D3.13 [2], respectively. Based on these requirements, a number of tests cases were derived.

Following SYNERGETICS' ambitions of demonstrating suitable retrofit options that allow a reduction in 35 %<sup>1</sup> in GHG emissions, viadonau provided a set of stakeholder's requirements to focus on achieving a design as close as possible to climate neutrality without hindering the operation of the vessel. At the same time, there are regulatory requirements mainly coming from ES-TRIN regulations, which require a minimum stopping, evasive and turning capability for the vessel. Simultaneously, the regulatory requirements are also linked to the stakeholder's requirements as the former need to be fulfilled so that the ship can be put into operation.

Whereas the emission reduction requirement is not strongly related to the dynamic behaviour of the vessel, the stopping, evasive and turning capability are. For this reason, two virtual models/digital twins were developed: a quasi-static and a dynamic model. This was done this way because for the test cases related to the reduction in GHG emissions, the transient states are not relevant as opposed to the test cases related to the stopping, evasive and turning capability, where its dynamic nature cover time-dependant phenomena such as inertia, acceleration and other transient effects for which a dynamic model is needed.

The models were developed using MARIN's v-ZEL, which is a repository of mathematical models of propulsion, power and energy systems of the vessel. The results of the simulations with the quasi-static model showed that when using bio-methanol (i.e., produced from biomass<sup>2</sup>) the new design with methanol-electric propulsion system can achieve approximately up to 80 % reduction in Well-to-Wake CO<sub>2</sub> equivalent emissions, reaching thus the ambition of achieving a 35 % in reduction of GHG emissions. However, it should be noted that this fuel has a limited feedstock. Therefore, it can be determined that the usage (and therefore availability for bunkering) of bio-methanol as energy carrier is crucial to achieve the 35 % target in reduction of GHG emissions in inland and coastal shipping.

In addition, the results of the dynamic simulations show that the new design will have a satisfactory stopping, evasive and turning capabilities, complying thus with the test case requirements and consequently with those from the ES-TRIN regulations.

---

<sup>1</sup> Goals of GHG reduction also defined in the Revised Rhine Navigation Act (Manheim Act) [3].

<sup>2</sup> Biomass from only residual forest wood and straw, as described by pathway #51 in deliverable D1.2 [5].



# 1. Introduction

Subtask 3.1.2 within Innovation Action SYNERGETICS aims to estimate the potential emission savings from implementing retrofit solutions in several demonstrators. The SYNERGETICS project has the ambition to demonstrate retrofitting solutions that allow to reduce GHG emissions (by at least 35 % compared to the original design), in line with the environmental objectives on the Revised Rhine Navigation Act (Manheim Declaration) of 2018 [3].

In order to evaluate the performance of the new design of Demonstrator 6 (Push boat for Austrian waterway operator viadonau), virtual models of the vessel were created. Virtual modelling allows to assess and verify the performance and reliability of a design before the production phase has started. In this way, better understanding of system behaviour can be achieved and design gaps can be identified while still being in an early design phase. With the aid of virtual modelling, costly mistakes can be avoided.

Figure 1-1 gives an overview of the W-model for product design in which virtual modelling is present. The left-hand side of the W corresponds to the initial conceptual design. For the power systems, this would correspond to the operational analysis, technology selection and conceptual design of the power and energy system, reported in deliverables D3.1 [1] and D3.13 [2]. In this stage the design requirements have been established as well as the size and characteristics of the main components. However, these may change depending on the outcome of the virtual modelling phase.

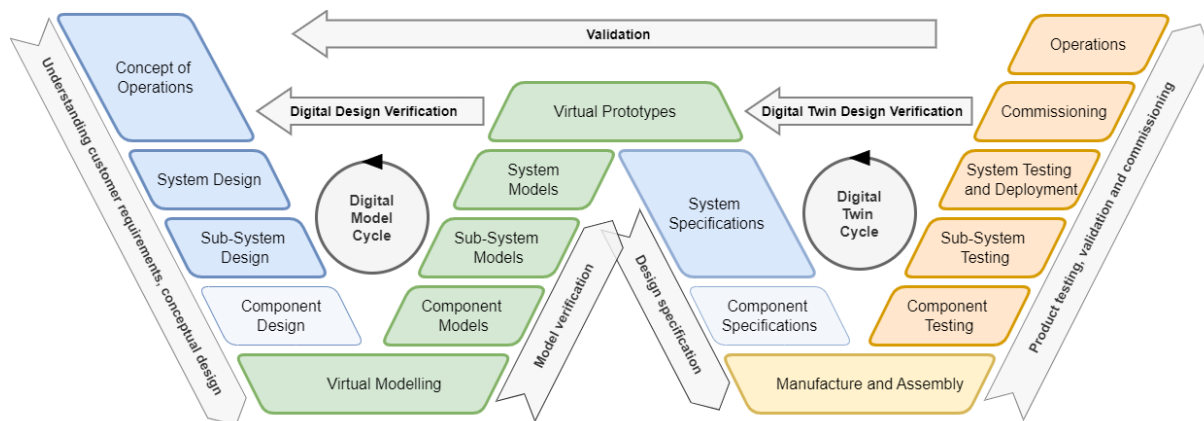


Figure 1-1: Schematic representation of the W-model for product design.

The middle part of the W corresponds to the virtual modelling phase of the design of the power and energy system, and it is the topic of this deliverable. In this phase a virtual model of the power and energy system is made, which is used to verify or refine the design requirements established during the conceptual phase. This allows to identify and solve potential issues in the design at an early stage, avoiding or limiting costly modifications at a later stage.

As the results of the concept design for Demo 6 were used as a starting point for the development of the virtual model, chapter 2 provides an overview of the work carried out during this stage.



## 2. Overview of the concept design

The Bad Deutsch-Altenburg is a push boat dedicated to the maintenance of the Danube River, owned by the Austrian waterway operator viadonau. The main particulars of the vessel are presented in Table 2-1. The boat is dedicated to waterway marking and maintenance of buoys and other aids to navigation to ensure the safe passage of vessel traffic through the Danube.

Despite being a low-emission vessel fitted with main engines compliant with EU Stage V NRE-v-6 emission regulations that can run on HVO100, viadonau is interested in exploring new concepts to reach lower emission levels for its future push boats.

Table 2-1: Main particulars of the Bad Deutsch Altenburg.

Characteristic	value
Ship type:	Push boat
Propulsion type	Diesel direct
Length over all	22.15 m
Length between perpendiculars	20.54 m
Beam, moulded	5.40 m
Beam, maximum	5.60 m
Depth, to main deck	2.25 m
Draught, design	1.10 m
Draught, maximum	1.20 m
Draught, ballast (Tf/Ta) <sup>3</sup>	1.116 /1.125 m
Deadweight, at maximum draught	11.00 t
Displacement, at design draught	73.40 t
Displacement, at maximum draught	82.98 t
Air draught above CWL	5.85 m
Speed (at 7 m draught and 90 % MCR)	19.9 km/h

Within the SYNERGETICS project, an operational analysis, technology selection and conceptual design of the power and energy system was conducted to study which power and energy concept was most suitable for the future viadonau push boat, which aims to have a lower emission level than the Bad Deutsch-Altenburg. The operational analysis and technology selection can be found in deliverable D3.1 [1]; the conceptual design of the power and energy system in deliverable D3.13 [2]. The following sections give a short overview of the work carried out for this demonstrator, which was used to develop the virtual model of the push boat.

<sup>3</sup> 10 % provisions and fuel, 80 % waste water, 3 crew members



## 2.1 Operational Analysis overview

As a first step of the concept design, the typical operations of the push boat were identified and analysed. Specifically, the following Bunker Independent Operations were defined:

- BIO I (round trip from Bad Deutsch-Altenburg to Krems an der Donau);
- BIO II (maintenance of Danube River/waterway marking);
- BIO III (Bathymetric survey)

Table 2-2 shows an overview of the three Bunker Independent Operations. For the verification of the new propulsion, power and energy conceptual design, BIO II (Maintenance of the Danube River) was used, as it was indicated by the ship operator (viadonau) as the most frequent operation for this vessel.

Table 2-2: Overview of the operational analysis

	BIO I	BIO II	BIO III
Autonomous range [km]	227	36.7	26.2
Endurance [h]	17.3	6	4
Total Energy [kWh]	3486	455	196
Average power [kW]	201.1	75.8	49
Max power [kW]	316.2	171.1	91.3

In BIO II, the ship departs with a barge from Bad Deutsch-Altenburg towards the west (upstream). After sailing 4 km, the vessel stops. There, waterway maintenance tasks are carried out for 30 minutes. Then the vessel with the barge sails upstream for another 5 km to arrive to another location and carries out a task related to waterway marking, for a period of time of 30 minutes. After these tasks are performed, the ship with the barge continues sailing 8 km upstream to another location where waterway maintenance tasks are performed for another 30 minutes. When these tasks are concluded, the ship with the barge sails downstream 8 km to another location where waterway markings are deployed/retrieved. This operation lasts for about 30 minutes. Ultimately, after this task has ended, the ship and the barge sail for another 10 km downstream to come back to Bad Deutsch-Altenburg. Figure 2-1 shows the power time profile of BIO II.



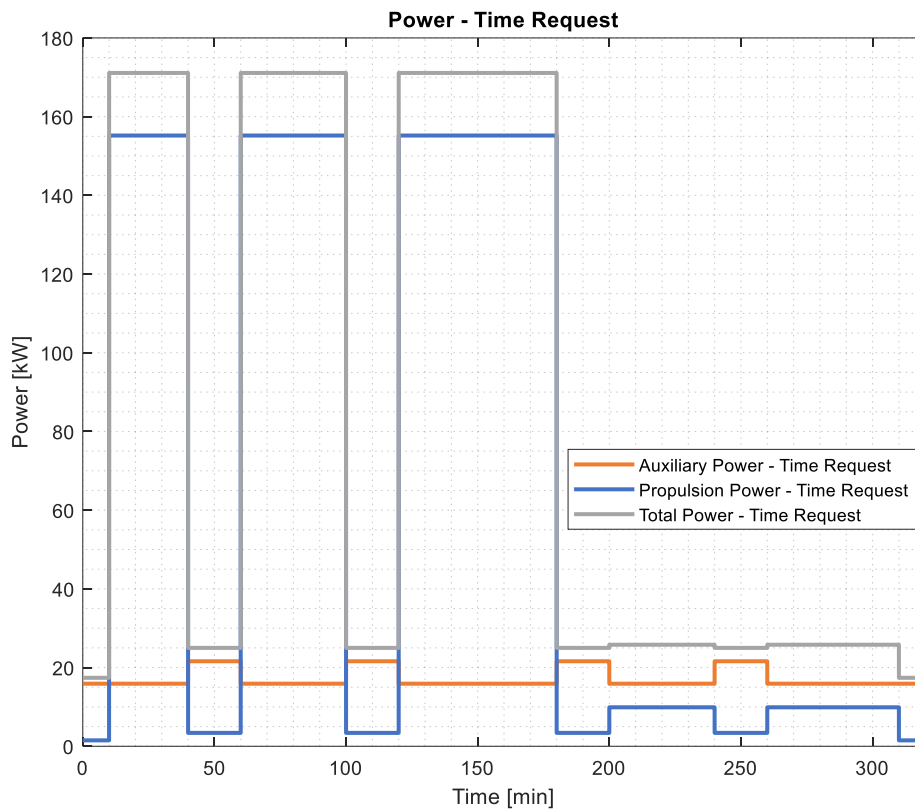


Figure 2-1: BIO II (Maintenance of the Danube River) power time profile



## 2.2 Propulsion, power and energy concept design

The single line diagram shown in Figure 2-2 summarises the results of the propulsion, power and energy concept design. The propulsion architecture was changed from a diesel direct one to a methanol electric one, two single fuel methanol gensets of different size were selected for the electric power generation on board of the vessel.

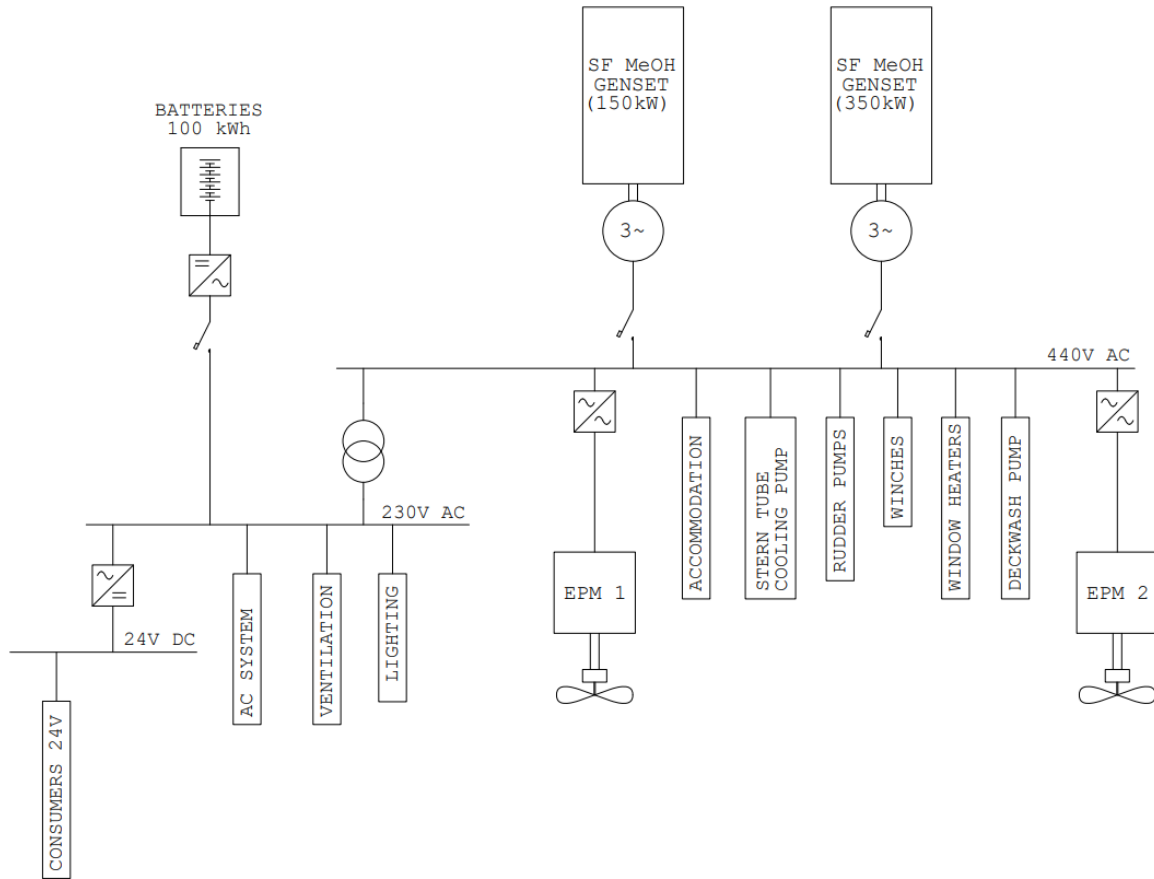


Figure 2-2: Single line diagram of the new propulsion, power and energy systems

The followings points summarise the main aspects of the propulsion system:

- Methanol fuel system: two 6 m<sup>3</sup> inerted tanks
- Propulsion system: electric propulsion motors (250 kW each)
- Electric power generation: two single fuel methanol genset (150 kW and 350 kW), one battery backup pack of 100 kWh



## 2.3 Test cases definition

During the development of the concept design, a requirements analysis was carried out to understand what is needed to achieve in terms of owner needs, as well as from a safety point of view according to the regulations. The complete requirement overview can be found in deliverable D3.13 [2]. For the definition of the test cases, two stakeholder requirements were considered:

- Req. 1: The new design shall be able to perform the "Maintenance of the Danube" operation.
- Req. 2: The "Maintenance of the Danube" operation shall be performed as close as possible to climate neutrality.

The feasibility of the first requirement was checked through a fuel consumption analysis and considering the tank size. To evaluate the climate neutrality, a comparison in terms of CO<sub>2</sub>eq emissions was made with the reference design. To do this, the following test cases were defined:

- Test case TC1: Quasi Static simulation of the reference design based on the "Maintenance of the Danube" operation
- Test case TC2: Quasi Static simulation of the new design based on the "Maintenance of the Danube" operation

During the operational analysis, test case *TC3 - Dynamic simulation to assess the performance of the new design* was defined. This test case was refined by test cases TC4, TC5 and TC6, explained below.

From the regulatory analysis the following ES-TRIN requirements were considered:

- ES-TRIN Article 5.07: Vessels and convoys shall be able to stop facing downstream in good time while remaining adequately manoeuvrable;
- ES-TRIN Article 5.09: Vessels and convoys shall be able to take evasive action in good time. That capacity shall be proven by means of evasive manoeuvres carried out within a test area as referred to in Article 5.03;
- ES-TRIN Article 5.10: Vessels and convoys with a length L of not more than 86 m or with a breadth B of not more than 22.90 m shall be able to turn in good time. That turning capacity may be replaced by the stopping capacity referred to in Article 5.07. The turning capacity shall be proven by means of turning manoeuvres against the current.

To verify these requirements and assess the dynamic performance of the new design, the following test cases were defined:

- Test case TC4: Dynamic simulation of the new design accelerating to maximum speed. Once the maximum speed is reached, a crash stop manoeuvre is performed;
- Test case TC5: Dynamic simulation of the new design performing an evasive action considering the river width.
- Test case TC6: Dynamic simulation of the new design performing a turning circle.

The first two test cases have been performed as a quasi-static simulation. This means that the system is modelled as passing through a sequence of equilibrium states so slowly that dynamic effects are neglected. This is done because for these two test cases the transient states are not relevant. The other three test cases have a dynamic nature as they cover time-dependant phenomena such as inertia, acceleration and other transient effects. Therefore, a dynamic model to represent the vessel is needed for these test cases. The test cases are described in more detail in sections 2.3.2.1, 2.3.2.2 and 2.3.2.3. The test cases have been conducted for a water depth of 7 m and, for some dynamic test cases, with a current of 5.6 km/h. This water depth and current correspond to the mean values encountered at MWL<sup>4</sup> in the river sections where the ship will sail, defined during the operational analysis.

---

<sup>4</sup> Mean Water Level, i.e., the average water level measured at a water gauge over a specific time period.



### 2.3.1 Quasi-static test cases

For the quasi-static test cases, the river maintenance operation is simulated using only the power-time chart for the maintenance of the Danube River shown in Figure 2-1. This power profile defines the propulsion and auxiliary power that the power system needs to supply at a certain time interval, and it is independent of the system architecture. The power request is subsequently converted into an engine fuel consumption depending the system architecture. The losses in the power distribution system are dependent of the architecture, as depicted in Figure 2-3. In Table 2-3 the efficiency values of the main components of the power system used for the simulations are listed. The calculations were made considering the power transformation efficiency chain in combination with the engine fuel consumption maps.

Figure 2-4 and Figure 2-5 shows the calculation chain of the two system architectures.

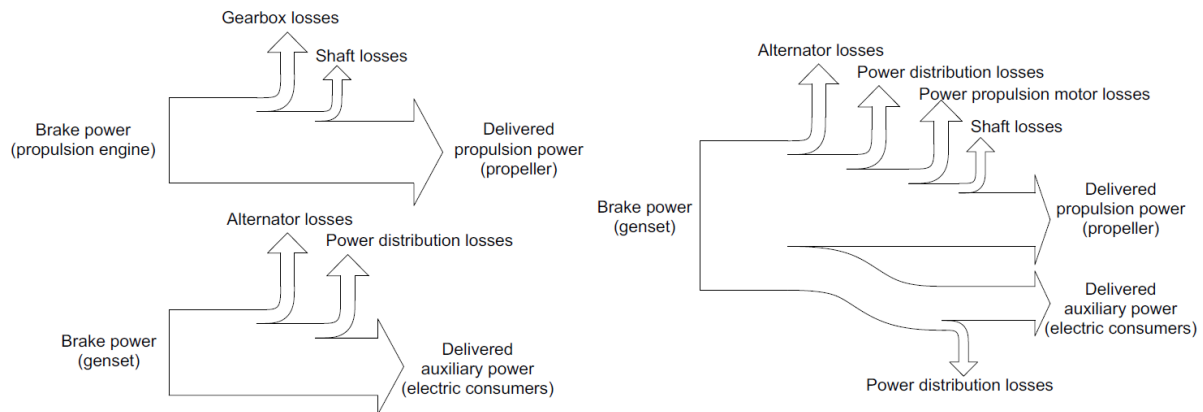


Figure 2-3: Overview of the power losses for the reference diesel direct (left) and new methanol electric (right) system architecture.

Table 2-3: Assumed components efficiency.

Component	Efficiency
Generator	95 %
Electric Machines	95 %
Main Grid	99 %
Secondary Grid	99 %
Gear Box	96 %



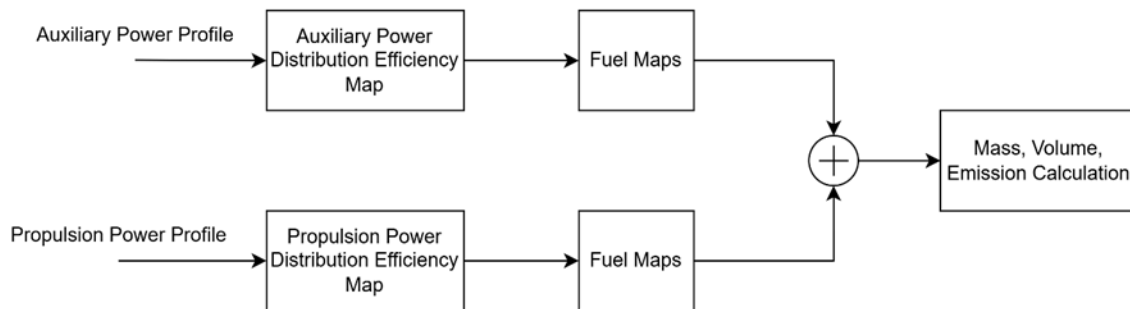


Figure 2-4: Diesel direct quasi static model calculation chain.

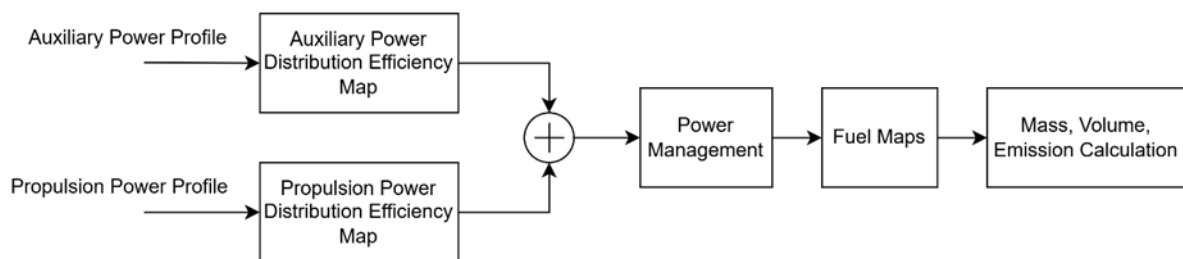


Figure 2-5: Genset electric quasi static model calculation chain.

Power Management block on Figure 2-5 represents a control algorithm that identifies, depending on the mechanical power requested by the engines, the number of gensets to switch on. The calculations of the CO<sub>2</sub> emissions (Well-to-Tank and Tank-to-Wake) have been executed using emission factors which give the carbon dioxide emissions per energy content (gCO<sub>2</sub>eq/MJ).

### 2.3.1.1 Test case TC-1: Quasi Static simulation of the reference design based on the “Maintenance of the Danube” operation

In this test case the river maintenance operation is simulated using the diesel direct architecture of the reference vessel, and therefore a diesel direct architecture with diesel and HVO as energy carrier is used.

### 2.3.1.2 Test case TC-2: Quasi Static simulation of the new design based on the “Maintenance of the Danube” operation

In this test case the river maintenance operation is simulated using the architecture presented in Figure 2-2 with MD97 as an energy carrier.



## 2.3.2 Dynamic test cases

### 2.3.2.1 Test case TC-4: Stopping capacity

In this test case the stopping capacity of the push boat sailing with the barge will be evaluated. Instruction ESI-II-3 in ES-TRIN establishes that the stopping capacity in relation to the water shall be demonstrated over a maximum distance measured in relation to the ground. For the push boat of Demo 6 (vessels and/or convoys less than 110 m in length), the maximum distance covered (track reach) must be equal or less than 480 m under the following standard conditions:

- Ship sailing downstream in flowing water with a current velocity of 1.5 m/s (5.4 km/h)
- Initial speed of 13 km/h
- Keel clearance equal to at least 20 % of the draught but not less than 0.50 m

Annex 1 of instruction ESI-II-3 indicates that the results of the stopping manoeuvre should be presented in a diagram presented similar to the one shown in Figure 2-6. The most important points of the manoeuvre marked in this diagram are:

- A stop order
- B propeller stopped
- C propeller in reverse
- D ship speed in relation to the water equal to zero
- E ship speed in relation to the water equal to zero

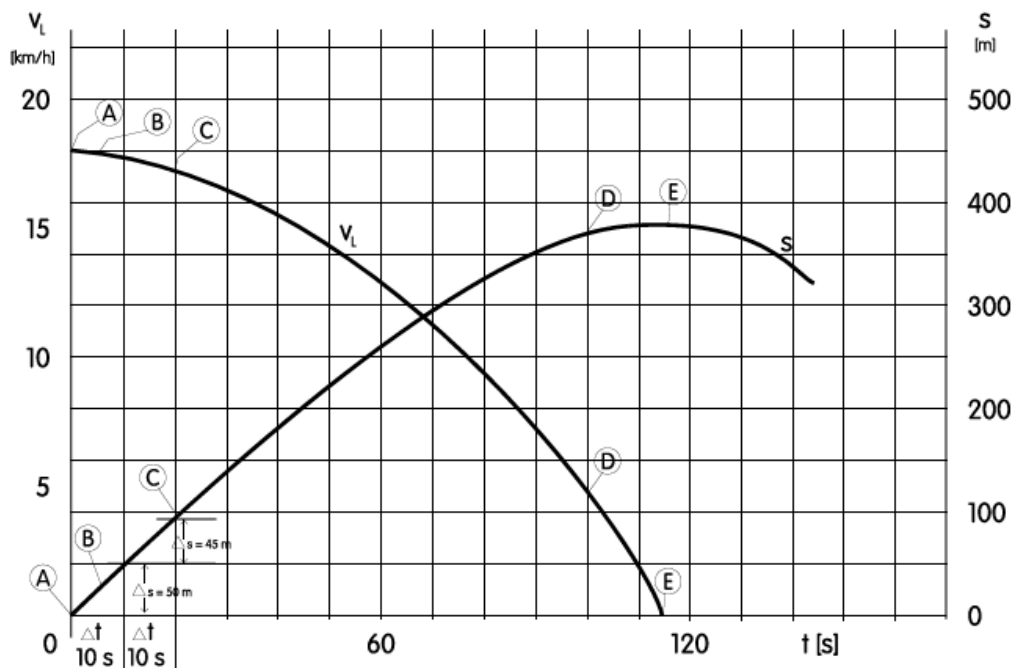


Figure 2-6: Example of diagram of the distance covered and speed of vessel during the stopping manoeuvre.

If the standard stopping manoeuvre conditions described above are not met, the stopping distance measured should be corrected to the standard conditions. To avoid additional corrections and allow a direct evaluation of the results, in this test case the following boundary and initial conditions were set:

- Ship sailing downstream with a speed over ground of  $V_s = 18.4$  km/h
- Current velocity of 1.5 m/s (5.4 km/h)
- Initial ship speed through the water of 13 km/h
- Water depth 7 m (keel clearance greater than 20 % of the draught)



### 2.3.2.2 Test case TC-5: Capacity for taking evasive action

During this test case the capacity for taking evasive action was evaluated following the procedure described in instruction ESI-II-4 of ES-TRIN, which specify that the evasive manoeuvre shall be conducted in the following conditions:

- Vessel or convoy underway sailing at a constant speed of 13 km/h in relation to the water
- Keel clearance equal to at least 20 % of the draught but not less than 0.50 m

The sequence of the operation, presented graphically in Figure 2-7, shall be as follows:

1. With the vessel or convoy under way at a constant speed of  $V_0 = 13$  km/h in relation to the water, at the start of the manoeuvre (time  $t_0 = 0$  s, turning speed  $r = 0^\circ/\text{min}$ , rudder angle  $\delta = 0^\circ$ , engine speed kept constant), evasive action to port or starboard is to be initiated by putting across the helm.
2. Rudder is set to an angle  $\delta$  at the start of the manoeuvre and is maintained until the value  $r_1$  of the turning speed  $r_1$  is reached. When the turning speed  $r_1$  is reached, the time  $t_1$  shall be recorded and the rudder set to the same angle on the opposite side so as to stop the turn and commence turning in the opposite direction
3. When the turning speed  $r_2 = 0$  is reached, the time  $t_2$  shall be recorded. When the turning speed  $r_3$  is reached, the rudder shall be set in the opposite direction to the same angle  $\delta$ , so as to stop the turning movement. The time  $t_3$  shall be recorded.
4. When the turning speed  $r_4 = 0$  is reached, the time  $t_4$  shall be recorded and the vessel or convoy shall be returned to its original course.

The manoeuvre shall be executed at rudder angles of  $\pm 20$  and  $\pm 45$  degrees.

Consequently, following the conditions required for this manoeuvre the following boundary conditions were used in the simulation of test case TC5:

- Ship speed through the water  $V_0 = 13$  km/h
- Water depth  $h = 7$  m
- Draught  $T = 1.1$  m (maximum deadweight condition)

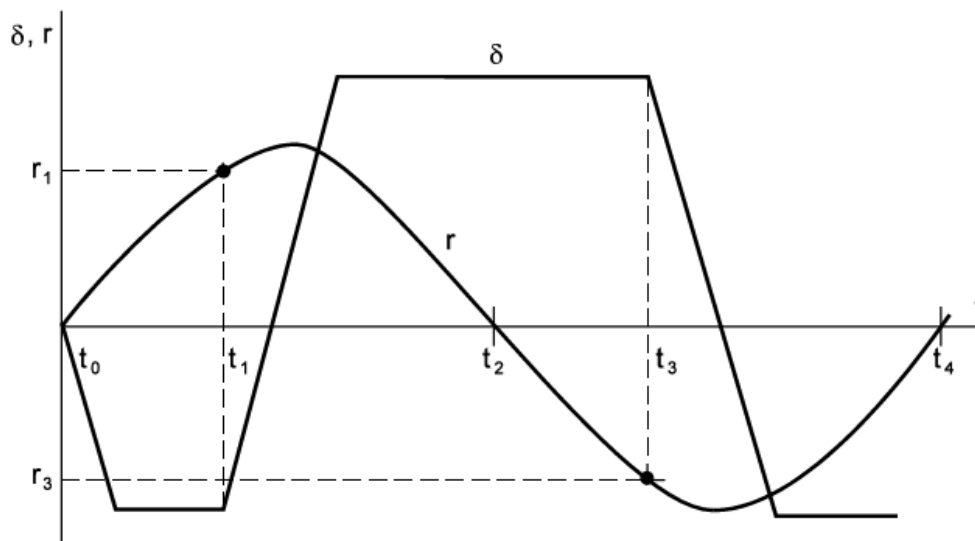
According to ES-TRIN ESI-II-4, for this type of vessel<sup>5</sup> for a  $h/T$  ratio of 8.75, the limit values from Table 2-4 will be required for the evasive manoeuvre for this vessel.

Table 2-4: Limit values allowed for the evasive manoeuvre performed in test case TC5.

	Rudder angle $\delta = 20^\circ$	Rudder angle $\delta = 45^\circ$
$r_1 = r_3$ [ $^\circ/\text{min}$ ]	20	28
$t_4$ [s]	110	110

<sup>5</sup> Type 1: All motor cargo vessels, motor tankers, passenger vessels and motorized floating equipment; single in-line convoys  $L \times B \leq 110 \text{ m} \times 11.45 \text{ m}$





- $t_0$  = Start of evasive action manoeuvre
- $t_1$  = Time to reach turning speed  $r_1$
- $t_2$  = Time to reach turning speed  $r_2 = 0$
- $t_3$  = Time to reach turning speed  $r_3$
- $t_4$  = Time to reach turning speed  $r_4 = 0$  (end of evasive action manoeuvre).
- $\delta$  = Rudder angle [°]
- $r$  = Turning speed [°/min]

Figure 2-7: Diagram of the evasive action manoeuvre described in instruction ESI-II-4 of ES-TRIN.

### 2.3.2.3 Test case TC-6: Turning capacity

According to the ES-TRIN regulations, the turning capacity of vessels and convoys whose length does not exceed 86 m and width does not exceed 22.9 m shall be considered sufficient when, during an upstream turning manoeuvre with an initial speed in relation to the water of 13 km/h, the limit values for stopping facing downstream established in instruction ESI-II-3 are complied.

In essence, this means that if the vessel/convoy satisfies the limit values of the stopping capacity test (test case TC-4), the turning capacity for the vessel/convoy is deemed as sufficient. As this is a rather vague definition, to evaluate the turning capability of the new push boat a turning manoeuvre was conducted under the following conditions:

- Ship sailing upstream<sup>6</sup> at maximum speed
- Current velocity of 1.5 m/s (5.4 km/h)
- Water depth 7 m (keel clearance greater than 20 % of the draught)

The sequence of the operation, depicted in Figure 2-8, will be as follows:

- 1) The vessel starts at zero speed, with zero degrees rudder and yaw angles, and accelerates to reach maximum speed.

<sup>6</sup> Manoeuvre conducted against the current as specified in ES-TRIN Article 5.10



- 2) Ship reaches maximum speed (i.e., equilibrium speed at 100 % MCR of propulsion power). For the rest of the test the propulsion motors will run at 100 % MCR.
- 3) Once the maximum speed is reached, the rudders are turned 35 degrees to one side.
- 4) When the ship has completed two complete turns, the rudder angle is set back to zero degrees

In this test the Advance, Transfer, Tactical diameter and Turning diameter will be measured.

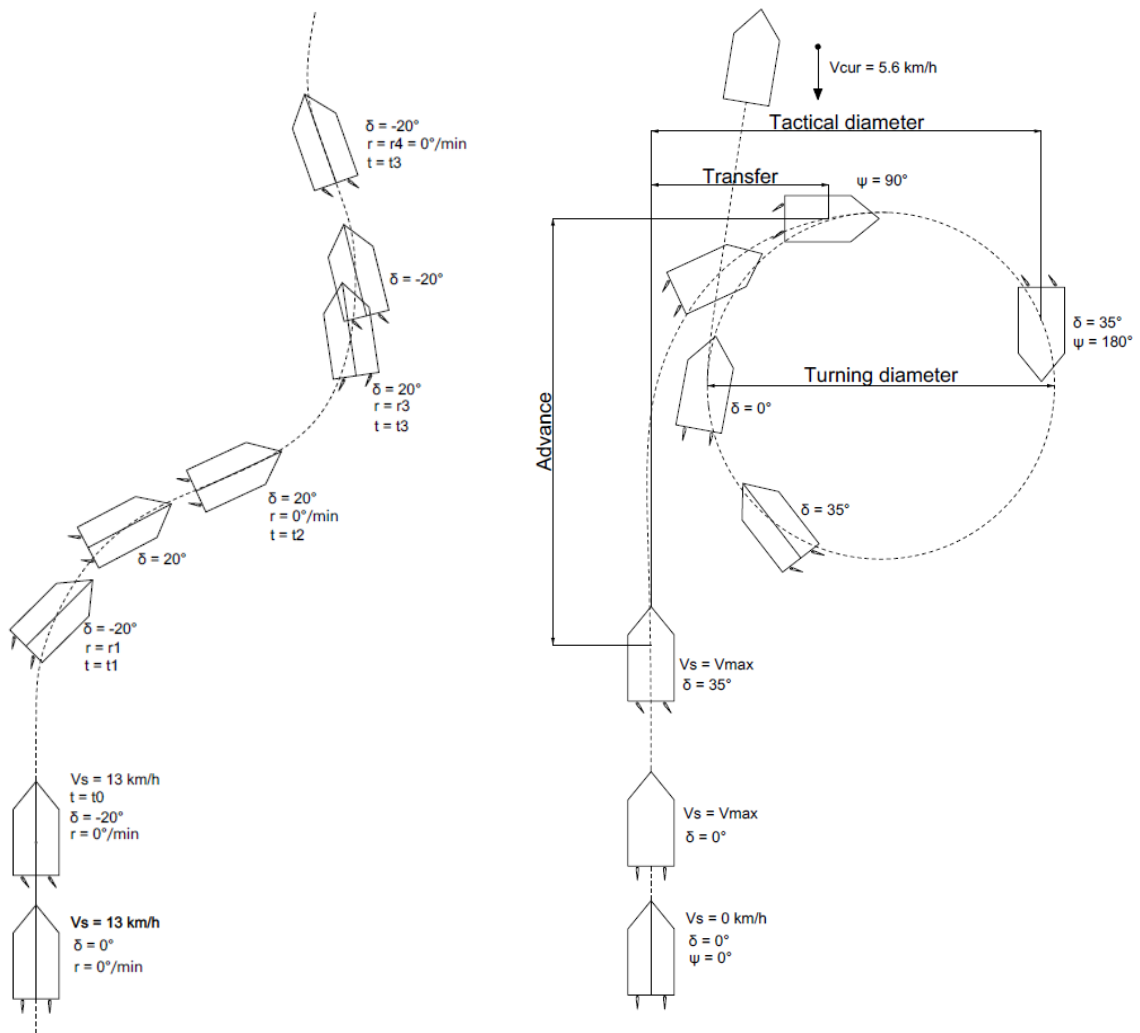


Figure 2-8: Schematic representation of the test sequence to be followed in test case TC-5 (left) and TC-6 (right). Barge has not been included in the drawing.



### 3. Propulsion, Power and Energy system modelling

The virtual model was developed using MARIN’s virtual Zero Emission Level (v-ZEL), which is a repository of mathematical models used to represent the propulsion, power and energy components within a ship. The v-ZEL components are defined as blocks and are linked using the Simulink environment.

In the following sections the models used for the quasi-static and dynamic simulations are described.

#### 3.1 Virtual model of the power systems for quasi-static simulations

The quasi-static model was developed to evaluate test cases 1 and 2, which aim to evaluate the climate neutrality of the new power and energy system compared to the current design as benchmark. For such, the following architectures were included in the model:

- **Reference:** Diesel direct propulsion with compression ignited ICEs running on biodiesel HVO100.
- **New design:** Methanol electric propulsion with single fuel compression ignited Methanol ICEs. Bio-methanol was used for the evaluation of the emissions.

The calculation chain shown in Figure 1-1 and Figure 3-2 were implemented using Matlab Simulink Software.

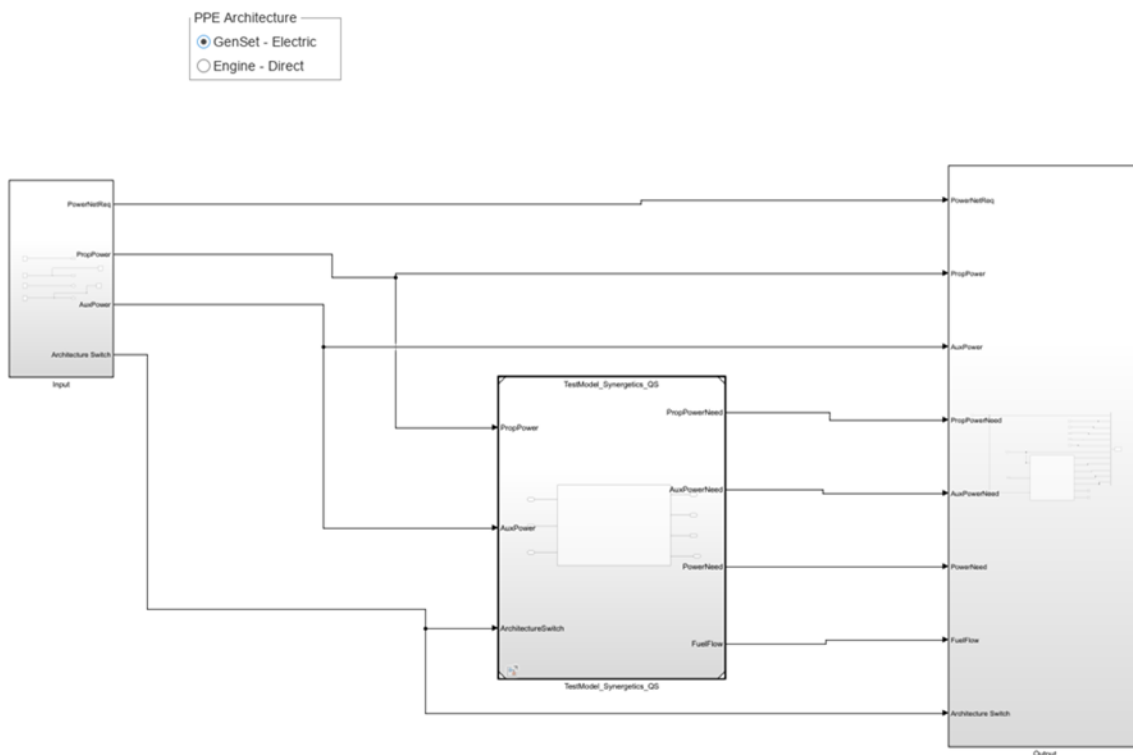


Figure 3-1: Simulink Model used for the quasi-static simulations.



As shown in Figure 3-1, the model architecture was divided into the following main blocks:

- **Input.**
  - in which the Power- Time Request from the operational profile is implemented
- **Test Model.** The test model, represented by the middle block in Figure 3-1, and in more detail in Figure 3-2, calculates the following parameters:
  - The mechanical power requested to the ICEs. In case the architecture selected (see radio button on Figure 3-1 top left) is Engine – Direct, the propulsion and auxiliary power requests are converted individually, into a propulsion mechanical power request (PropPowerNeed) to the propulsion engines and to auxiliary mechanical power request (AuxPowerNeed) to the auxiliary engine. In case of Genset – Electric architecture, the propulsion power and auxiliary requests are converted into total mechanical power request to ICEs.
  - The Diesel and MD97 fuel flow rates.
- **Output:** which calculates the data needed (Fuels Mass and Volume, CO<sub>2</sub> emission).

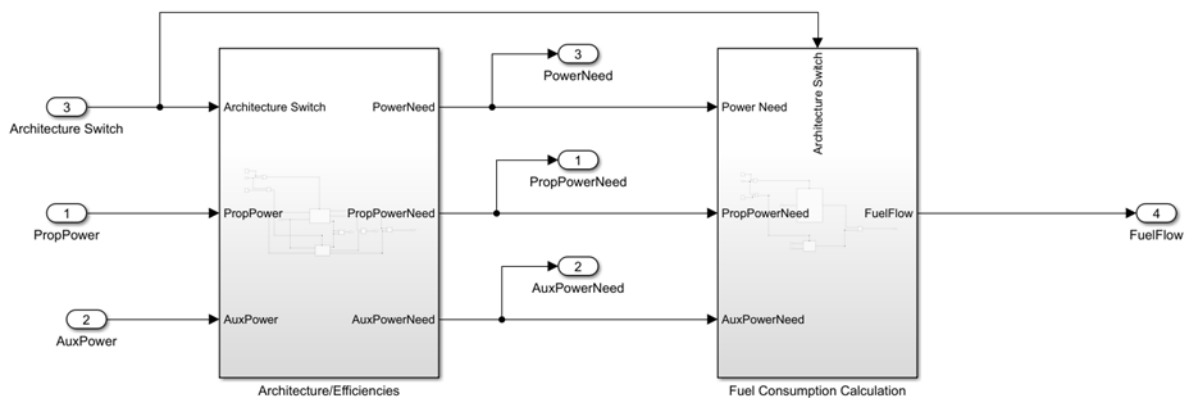


Figure 3-2: Quasi-static test model.

As the time step of the simulation is much smaller than the total simulation period (hours), the introduced error is neglected. The simulation settings of the Simulink Model are given in Table 3-1.

Description	unit	QS Test Model
Solver Type	-	Fixed-step
Solver	-	discrete
Step Size	s	1

Table 3-1 Simulation settings used for the quasi-static test model.



### 3.1.1 Fuel consumption maps

Figure 3-3 shows the maps used to calculate, on basis of a power request, the engines fuel mass flow rate. As specified in the graph legend, all lines, except the one related to the propulsion engine, refer to engines rotating at a constant speed. This is due to the fact that those engines are connected to a generator and, to keep the grid frequency constant, they need to run at constant speed. On the contrary, the propulsion engine fuel consumption map has been deduced on the basis of the mechanical propulsion power requested by the propeller.

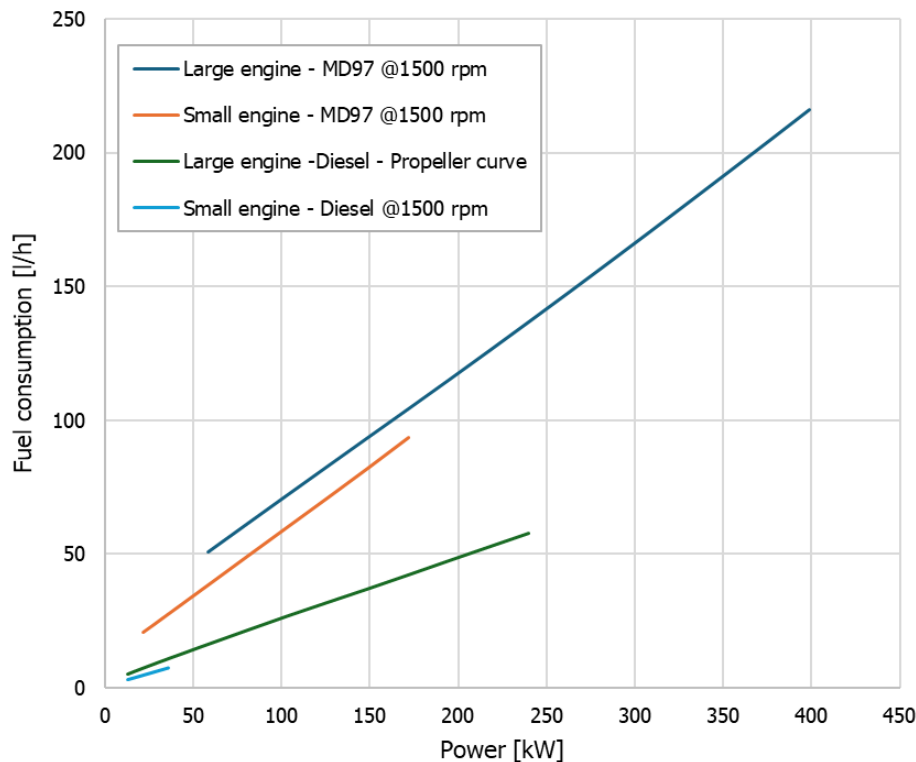


Figure 3-3: Fuel consumption maps.



### 3.1.2 Emissions calculation

For the evaluation of the emission reduction the following energy carriers were used:

- Test case 1 (reference): Diesel, HVO
- Test case 2 (new design): Bio-methanol.

The calculation was carried out considering the Lower Heating values (LHV) from Table 3-2. For the calculation of the emissions, the emission factors presented in deliverable D4.5 [4] were used. These correspond to the factors from EcoTransIt World 2024 for the diesel and HVO. Since methanol is not yet part of EcoTransIt study, the data collected and calculated in deliverable D1.2 [5] was used for the emission factors of bio-methanol, represented by pathway #51. The emission factors for the energy carriers are shown in Table 3-3 and Table 3-4.

Table 3-2: Lower Heating Value (LHV) of the fuels used in the simulations.

Fuel	LHV [MJ/kg]
Diesel	42.8
HVO	44
Methanol	19.9

Table 3-3: CO<sub>2</sub> equivalent emission factors used for the emission calculations.

	Well-to-Tank CO <sub>2</sub> eq WTT [kgCO <sub>2</sub> eq/kgfuel]	Tank-to-Wake CO <sub>2</sub> eq TTW [kgCO <sub>2</sub> eq/ kgfuel]	Well-to-Wake CO <sub>2</sub> eq WTW [kgCO <sub>2</sub> eq/ kgfuel]
Diesel	0.966	3.221	4.187
HVO	0.051	1.257	1.308
Bio-Methanol	1.430	Net zero	1.430



Table 3-4: NO<sub>x</sub> and PM emission factors used for the emission calculations.

	Well-to-Wake NO <sub>x</sub> emission [kgNO <sub>x</sub> /kgfuel]	Well-to-Wake PM emission [kgPM/kgfuel]
Diesel	1.673	0.295
HVO	0.00191	0.000153
Bio-Methanol	0.11287	0.01357

### 3.2 Virtual model of the new power system for dynamic simulations

The dynamic model of the power system used for the dynamic test cases was developed from the single line diagram of the new design developed during the conceptual design. As shown in Figure 3-4, a mathematical model was used to represent the main components of the power system.

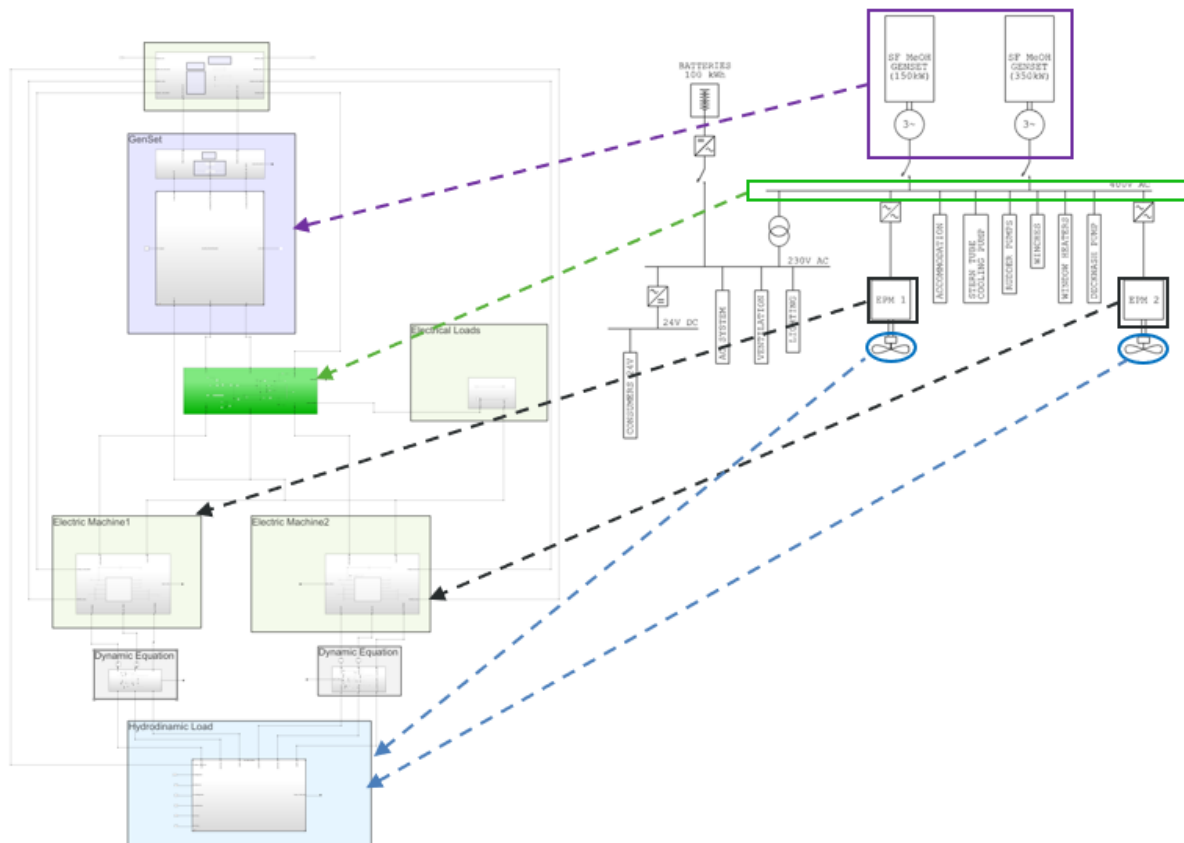


Figure 3-4: Comparison of the main components of the single line diagram (right) with those of the dynamic model (left) of the new power and energy system of the push boat, used for the dynamic test cases.



In addition to the mathematical models of the power systems, a hydrodynamic model was used to calculate the hydrodynamic loads experienced by the propellers during the operation.

### 3.2.1 AC Distribution System

For simplicity, the AC System was modelled using the following assumptions:

- neglecting Cables modelling
- neglecting Power Electronics Components: their presence and, of the previous ones, have been modelled considering energy losses (efficiency coefficients – see Table 2-3)

With these assumptions, the power balance equations are simplified only to the current balance, and the AC frequency, is calculated determining the engines rotational speed.

### 3.2.2 Genset Models

#### 3.2.2.1 Internal Combustion Engine (ICE) Models

Following on from the previous work packages, the specifications for the engine models were composed. Since the configuration for the push boat consisted of two different gensets, this was done for two engines. Although these engines are conceptually equal, their specifications differ. For that reason, two separate engine model configurations were needed. The smaller genset has an electric output of 150 kW, the larger one has 350 kW. Taken a generator efficiency of 95 % into account, and respecting a maximum continuous rating of 90 %, this resulted in engine-out power targets of 175 kW and 410 kW. Since the architecture is AC, a fixed speed of 1500 rpm was chosen for both sets.

Based on data from Scandinaos from deliverable D3.17 [6], and specifications from the base-engine manufacturer, a basic size was chosen for both engines. This resulted in a 5-cylinder 9.3 litre engine, and an 8 cylinder with 16.3 litre.

The single fuel engine methanol engine in this concept is running according to the diesel principle. This requires a dedicated fuel, MD97, which consists of 97 methanol and is refined with lubrication and an ignition enhancer. For modelling purposes, the properties of this specific fuel were compiled. Most important were the stoichiometric air fuel ratio, carbon mass fraction, density and energy density. In the MARIN engine model values of 6.64 kg/kg, 0.39, 0.820 kg/m<sup>3</sup> and 20 MJ/kg were used.

With these base numbers the engine model was parametrized to reach the desired output. This process starts with setting all basic (mechanical) parameters. Combining this with target boost pressure and

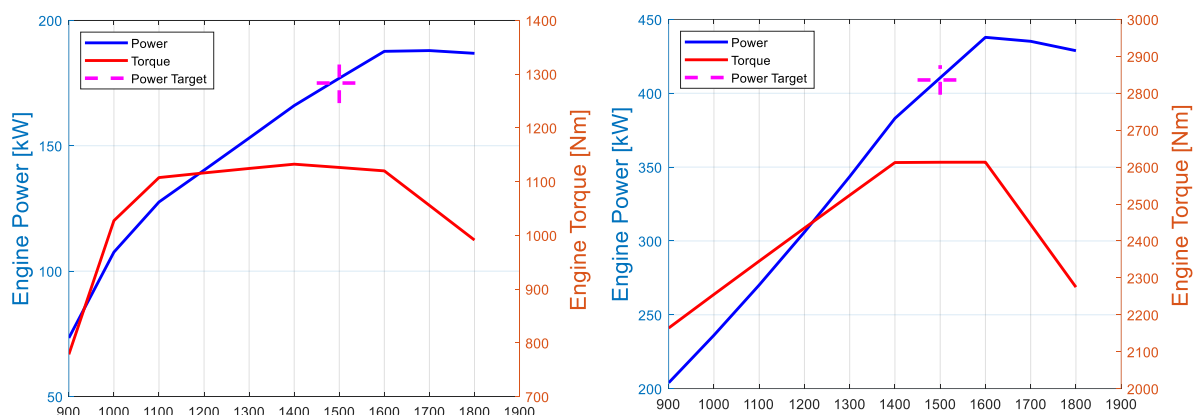


Figure 3-5: Power curves for the modelled 175 kW (left) and 410 kW (right) single fuel MD97 engines.

maximum allowable air fuel ratio's, gives a running model. The combustion profile, modelled by making



use of a double Wiebe curve, was kept equal to a diesel combustion, since this is the way, the fuel is used in this single fuel concept. After multiple iteration loops on boost level and turbocharger sizing, the following output was created.

Maintaining the net frequency via a speed control on ICE's could potentially bring to a net instability and a possible black out during power sharing. For that reason, the engines are controlled using a Droop Control Strategy (see Figure 3-6).

### 3.2.2.2 Alternator Model

The alternator has been modelled as an energy/power conversion between the ICE and the AC distribution system. In other terms, considering a constant voltage in the BUS, the ICE mechanical power is converted into current delivered in the BUS, considering the power losses in the alternator.

The resistive torque  $T_r$  applied to the ICEs, is calculated according the following formula:

$$T_r = \frac{P_{el}}{\eta_{Gen} \cdot \omega_{ICE}}$$

where

- $P_{el}$  = total electrical power requested by the power consumers at the BUS distribution system
- $\eta_{el}$  = generator system efficiency
- $\omega_{ICE}$  = ICE rotational speed

Consequently, the ICE rotational speed is calculated solving the following dynamic equation:

$$\dot{\omega}_{ICE} = \frac{T_{ICE} - T_r}{J_{eq}}$$

Where:

- $\dot{\omega}_{ICE}$  = ICE rotational acceleration
- $T_{ICE}$  = torque generated by ICE
- $J_{eq}$  = equivalent rotational inertia; i.e., sum of the ICE and Generator inertia reduced to the axis.

Once the rotational speed is determined, the net frequency  $f$  can be calculated as follows:

$$f = \frac{N_p \cdot \omega_{ICE}}{120}$$

where:

- $N_p$  = generator number of poles
- $\omega_{ICE}$  = ICE rotational speed, in rpm



### 3.2.2.3 Gensets control logic - Droop Control

By measuring the engine rotational speed (or frequency), each engine control system reacts injecting the fuel quantity expressed as load percentage. This is controlled by the so-called droop lines. Figure 3-6 shows the droop lines used for the dynamic model, which refer to a stationary condition in which the mechanical power  $P_{ICE}$  generated by the ICEs is equal to the mechanical power absorbed by the two generators. In the equilibrium state, the following equation is satisfied:

$$P_{ICE_1} + P_{ICE_2} - P_{el} / \eta_{Gen} = 0$$

where:

- $P_{el}$  is the total electrical power requested by the power consumers at the BUS distribution system;
- $\eta_{Gen}$  is the generator efficiency
- $P_{ICE_1}$  is the mechanical power delivered by the ICE of genset 1
- $P_{ICE_2}$  is the mechanical power delivered by the ICE of genset 2

If a transient load occurs, the two engines will react according the droop lines, generating together more or less power (frequency droop or rise) in order to bring the system in a new operation point where the equation above is again verified.

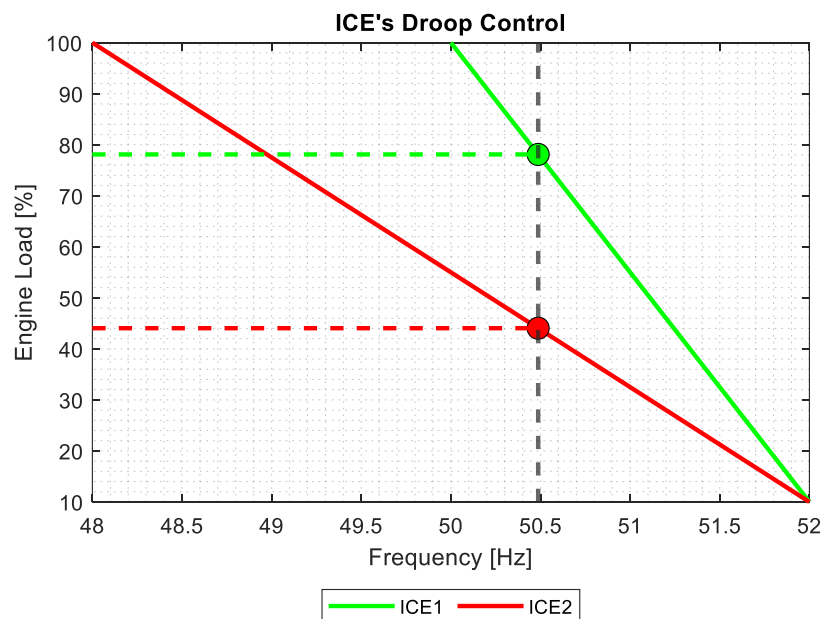


Figure 3-6: Droop lines of the methanol gensets used for load sharing the dynamic simulation.

In the model, the droop lines strategy is completely configurable (frequency range and lines inclination) depending the number of the gensets connected to the grid. In that way it is possible to optimise, knowing the ICEs characteristic curves, the efficiency of the power system for a specific request of power.

To connect the genset to the grid it is necessary to execute the following sequence:

1. Switch ON the ICE
2. Once the ICE is ON, according the coupled generator, bring its rotational speed to the correspondent net frequency



3. Execute a voltage adjustment according the net one
4. Execute a frequency phase synchronization
5. Close the breaker
6. Once the genset is connected, control the ICE via a Droop Control

Figure 3-7 shows an example of how the connecting procedure is implemented in the model. Considering how the AC distribution system and the generators have been modelled, the voltage adjustment procedure has been neglected and the synchronization has been implemented as a delay time before the generator is connected to the grid. This delay time has not been modelled simply as a waiting time, but as the time needed for the rotational speed to reach a stable value and equal (within a bandwidth) to the target value.

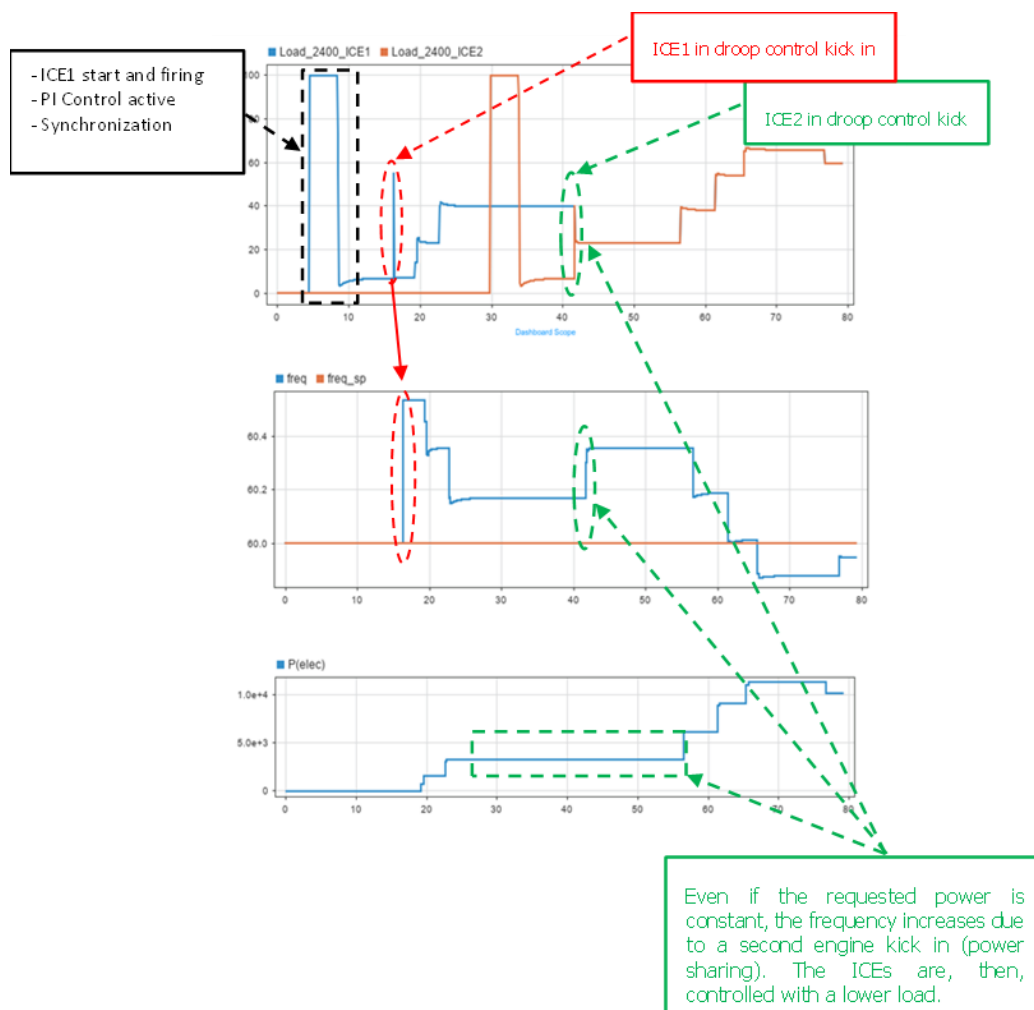


Figure 3-7: Example of genset synchronization procedure.



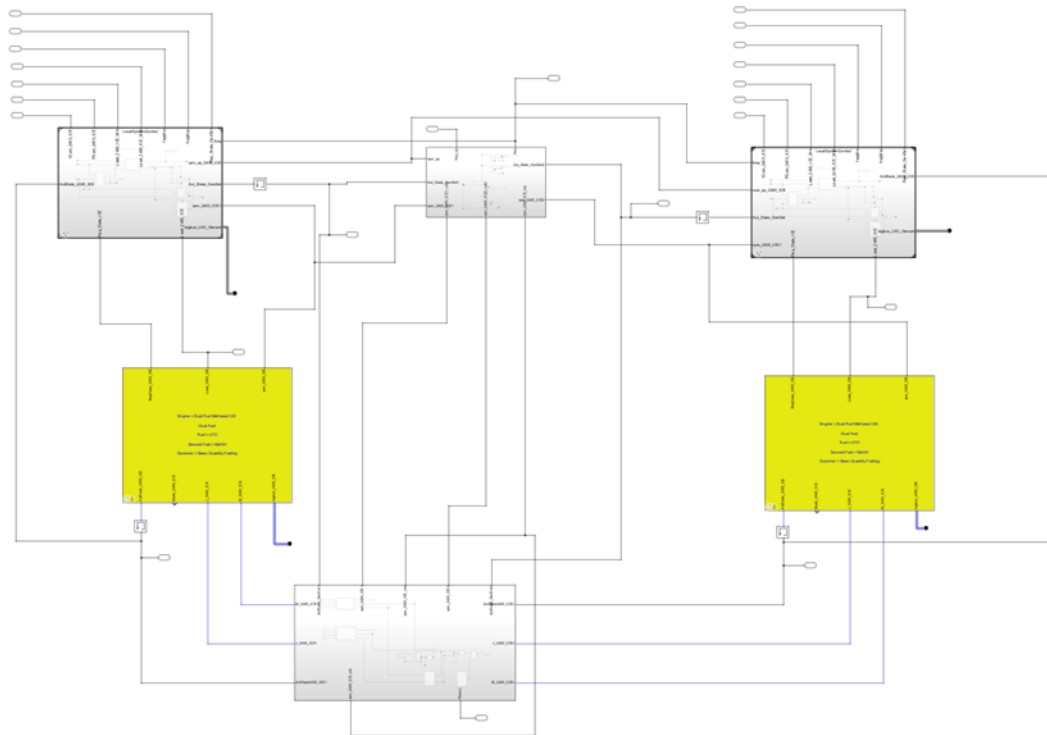


Figure 3-8: Overview of the v-ZEL dynamic model used for the methanol gensets.



### 3.2.3 Propulsion motors

The propulsion system of the new design of the push boat encompasses two permanent magnet assisted synchronous reluctance drive motors controlled by a torque controller. Mechanical power from the electric motors is transferred to the shaft lines. The ship has two of these motors to drive the two propellers. Figure 3-9 shows the modelled single quadrant operation characteristics curves of these motors. Those values, with different sign, have been also used for the other operational quadrants (e.g. negative rotational speed and positive power).

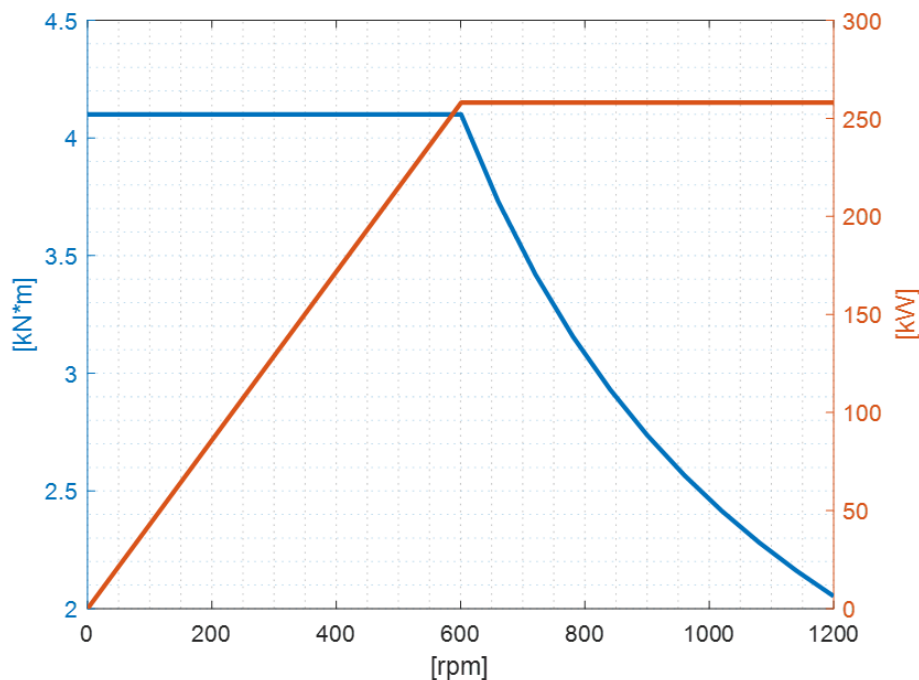


Figure 3-9: Characteristic curves (blue = torque; orange = power) used for the dynamic model of the electric motors used for propulsion.

### 3.2.4 Hydrodynamic model

In order to describe the hydrodynamic behaviour of the push boat, a hydrodynamic model was used. The model was developed using MARIN's eXtensible Modelling Framework (XMF). XMF is a C++ software toolkit on which all MARIN's fast-time and real-time simulation software is based. The XMF system reads the model from the file, loads the related dynamic content libraries and starts executing a time domain simulation. The mathematical model is based on a time-step solution of the system of coupled differential equations of motion.

Ship specific results from model experiments, semi-empirical methods (such as slender body and cross-flow drag theory), and linear frequency domain tools are typically used to model the hydrodynamics. Other elements such as rudders, propellers, thrusters, etc. are modelled in time domain, where generic solvers are used to solve the equations of motion. In the following subsections a short definition is given of the reference frame and the mathematical models of the components used for the hydrodynamic model.



### 3.2.4.1 Coordinate system

The origin of the coordinate system coincides with the centre of gravity of the convoy (ship+ barge), as depicted in Figure 3-10. The x-axis points in ship forward direction, y-axis to port side and z-axis is positive upward.

Ship displacements (surge, yaw and heave) are defined positive in the positive direction of the corresponding coordinate axes and rotations (roll, pitch and yaw) by mathematical positive (right-handed) rotations around the coordinate axes.

The rudder angle  $\delta$  corresponds to the angle between the ship longitudinal axis and the rudder chord. A positive rudder angle means that the rudder trailing edge is rotated towards the starboard side of the ship (leading the ship to turn to starboard at forward speed).

The propeller axis  $x_p$  points in ship forward direction.  $V$  is the ship velocity in the (horizontal) x-y-plane with the components  $u$  and  $v$  in x- and y-direction respectively. The drift angle  $\beta$  is defined as

$$\beta = \tan^{-1}\left(\frac{v}{u}\right)$$

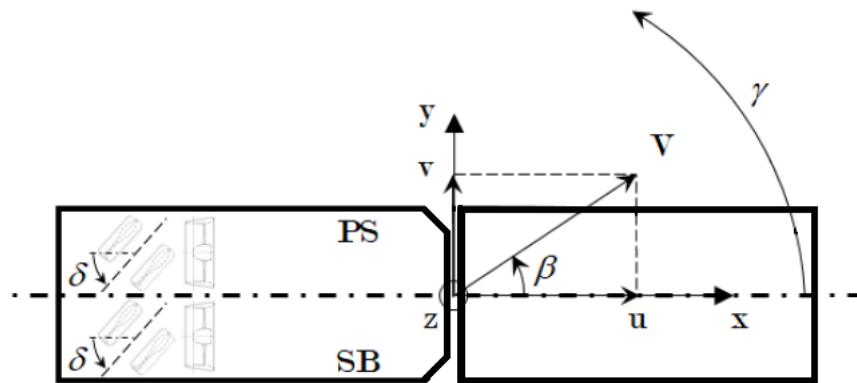


Figure 3-10: Ship-fixed coordinate system used for the simulations for the dynamic test cases.

### 3.2.4.2 Hydrostatics

The static equilibrium is dominated by the balance between weight and buoyancy. Due to the quasi-static motion, the balance can be disturbed by a shift of the position of the centre of gravity, a shift of the position of centre of buoyancy, and a change in the magnitude of the buoyancy. The linear hydrostatics model these effects and the influence on the ship stability, by determining a linearised stiffness matrix  $K_g$  at the centre of gravity (from a linear restoring matrix at the centre of floatation and a spring matrix at the centre of gravity) expressed in the form:

$$K_g = \begin{bmatrix} 0 & 0 & 0 & 0 & 0 & 0 \\ 0 & 0 & 0 & 0 & 0 & 0 \\ 0 & 0 & \rho g A & \Delta y \rho g A & -\Delta x \rho g A & 0 \\ 0 & 0 & \Delta y \rho g A & GM_t \rho g V + \Delta y^2 \rho g A & -\Delta x \rho \Delta y \rho g A & 0 \\ 0 & 0 & -\Delta x \rho g A & -\Delta x \Delta y \rho g A & GM_t \rho g V + \Delta x^2 \rho g A & 0 \\ 0 & 0 & 0 & 0 & 0 & 0 \end{bmatrix}$$



### 3.2.4.3 Resistance

The resistance was modelled using the resistance curves calculated for the speed power prediction during the operational analysis (see [1]).

### 3.2.4.4 Manoeuvring reaction forces

The manoeuvring reaction forces were modelled via coefficients multiplied by the motion derivatives (ship velocities). These coefficients fit captive manoeuvring model experiment results of similar ships that were tested at MARIN.

### 3.2.4.5 Propeller and duct open water characteristics

The propeller and duct mathematical model provides the forces of the propeller and duct as a function of the propeller loading and inflow angle. The propeller and duct model are based on the open water curve of the propeller and duct based on the Ka-series with a 19A-type duct.

Usually, a propeller operates in the range from zero speed up to where the thrust becomes zero. There are, however, a number of situations where additional data is needed to analyse the propulsive quantities of a ship's propeller, e.g. the torque and drag of a slowed down or even stopped propeller, the determination of the astern thrust, etc. As these situations might occur during the operation of the vessel, it is necessary to extend the open water characteristics to the conditions where the advance speed and/or the propeller rotation rate becomes negative. In order to answer these questions, the traditional open water diagram has to be extended over 4 quadrants. In Table 3-5 and overview of the conditions for each quadrant is given.

Table 3-5: Overview of the conditions that define the open water characteristics for four quadrants.

Quadrant No.	b	Speed of advance	Rotation rate
1	$0^{\circ} < \beta < 90^{\circ}$	+	+
2	$90^{\circ} < \beta < 180^{\circ}$	+	-
3	$180^{\circ} < \beta < 270^{\circ}$	-	-
4	$270^{\circ} < \beta < 360^{\circ}$	-	+

The open water characteristics used for the simulations, presented in Figure 3-11 and Figure 3-12, are function of the angle of advance  $b$ , defined as:

$$b = \text{atan}\left(\frac{V_a}{0.7\pi nD}\right)$$

where:

- $V_a$  is the speed of propeller relative to waterflow;
- $n$  and  $D$  are the rotational speed and diameter of the propeller, respectively.

The thrust and torque of the propeller can't be made non-dimensional as in the usual open water diagrams by division by the rotative speed squared because conditions occur where the rotation rate becomes zero. Therefore, different non-dimensional coefficients must be used  $C_T$  and  $C_Q$  with the following definitions:



$$C_T = \frac{T}{\left(\frac{\pi}{8} \rho D^2 (V_a^2 + (0.7 \pi n D)^2)\right)}$$

and:

$$C_Q = \frac{Q}{\left(\frac{\pi}{8} \rho D^3 (V_a^2 + (0.7 \pi n D)^2)\right)}$$

In addition, as shown in Figure 3-11 and Figure 3-12 the open water characteristics are defined for different inflow angles (0, ±20 and ±40 degrees). This way, the open water characteristics can cover all conditions that may occur during the simulations.

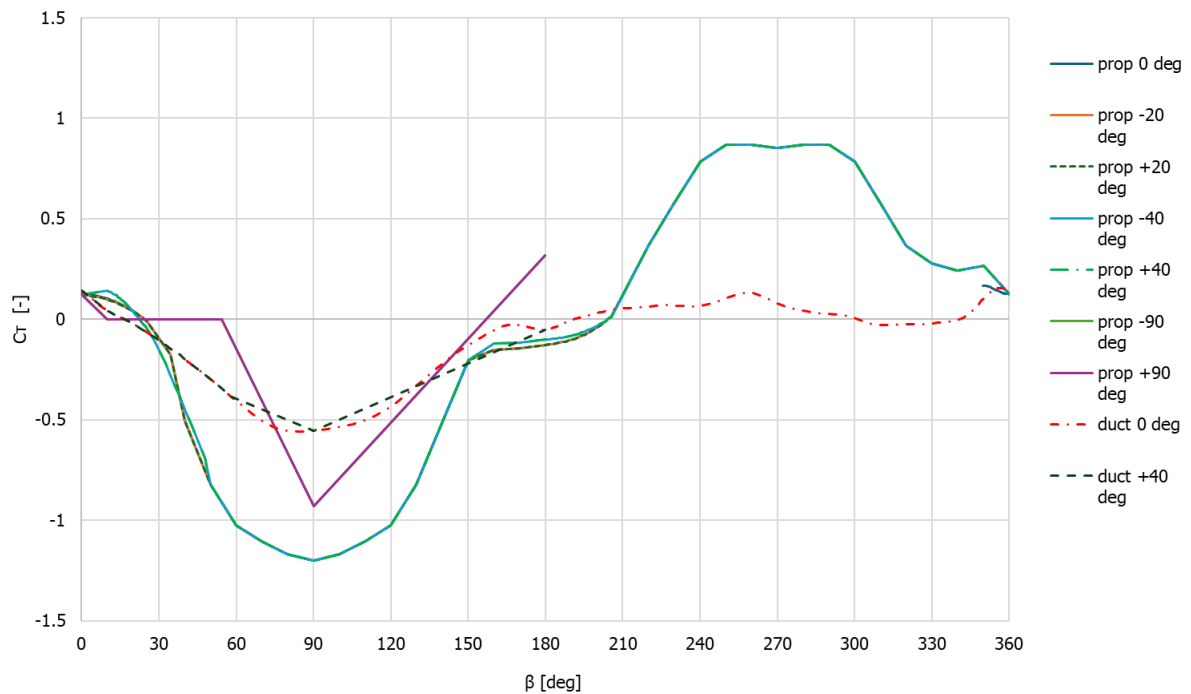


Figure 3-11: Thrust coefficient (CT) as function of the angle of advance ( $\beta$ ) and the inflow angle (0, ±20, ±40 and ±90 degrees).



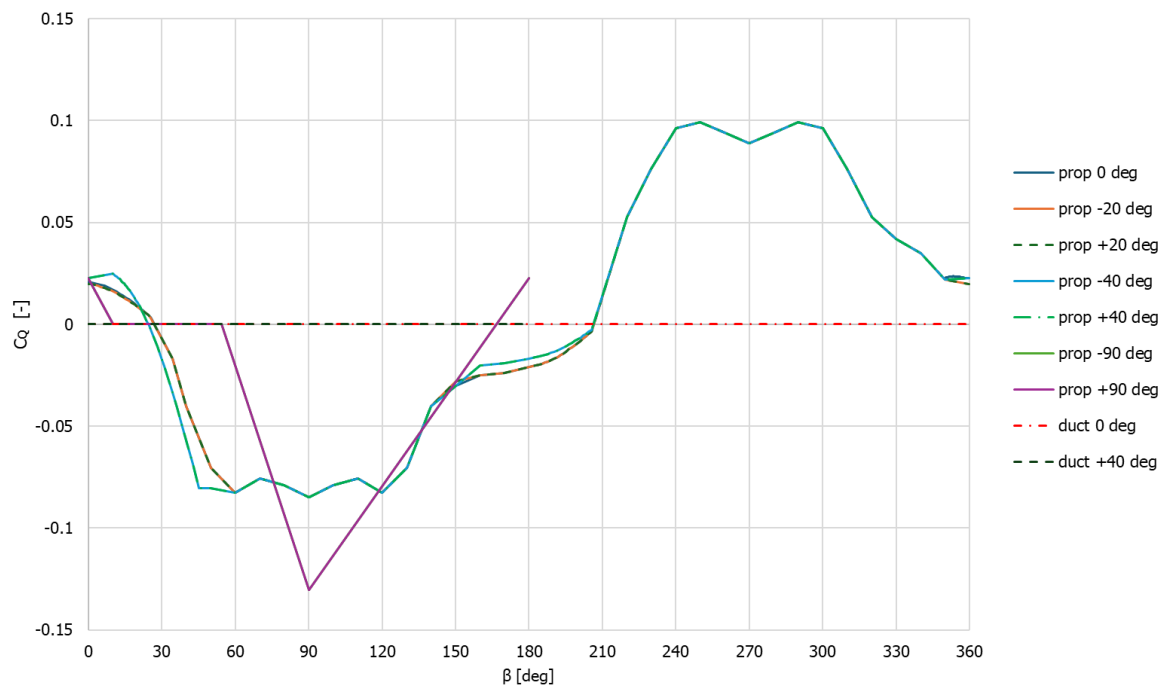


Figure 3-12: Torque coefficient (CQ) as function of the angle of advance ( $\beta$ ) and the inflow angle (0,  $\pm 20$ ,  $\pm 40$  and  $\pm 90$  degrees).

### 3.2.4.6 Wind forces and moments

The wind forces and moments acting on the vessel were modelled using the coefficients  $C_x$ ,  $C_y$  and  $C_n$ . These coefficients are dependent on the direction of apparent wind as shown in Figure 3-13. For such, the coefficients from similar vessels were used. With these wind coefficients the forces and yaw moment due to wind were calculated as follows:

$$X_w = C_x \frac{1}{2} \rho U A_x$$

$$Y_w = C_y \frac{1}{2} \rho U A_y$$

$$N_w = C_n \frac{1}{2} \rho U \frac{A_y^2}{L_{oa}}$$

Where:

- $U$  is the apparent wind speed;
- $A_x$  and  $A_y$  are the frontal and lateral area of the ship exposed to wind;
- $\rho$  is the density of the wind; and
- $L_{oa}$  is the length over all of the vessel.



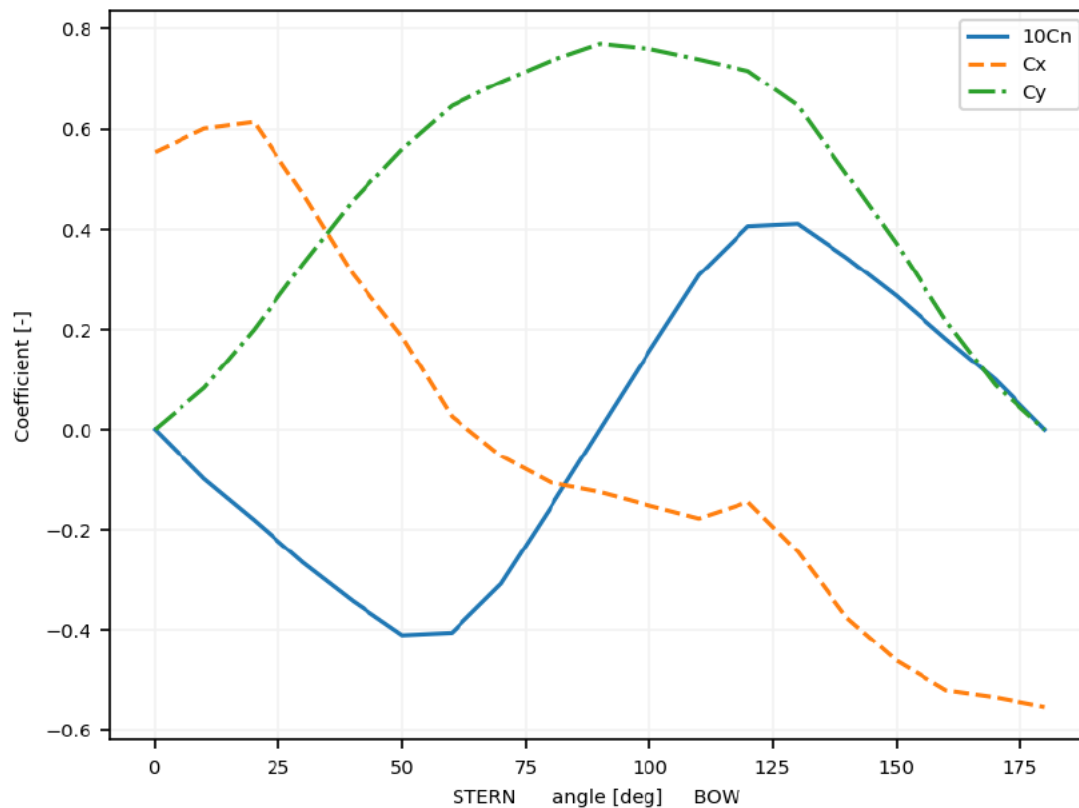


Figure 3-13: Wind coefficients used for the calculation of the wind force in longitudinal ( $C_x$ ) and transverse direction ( $C_y$ ), and the yaw wind moment ( $C_n$ ).

### 3.2.4.7 Rudder

For the rudder, the mathematical model described in [7] was used. This model provides the rudder reaction forces and moments.

The model is defined by the dimensions, location, and stock inclination angle in the  $y$ - $z$  plane. The model includes the interactions with the hull and a propeller. These interactions consist for instance of the effect of an accelerated inflow when positioned in a propeller slip stream, or the effect of a straightened inflow due to the presence of the hull. The mathematical model is based on lifting line and axial momentum (actuator disc) theory, with the implementation of empirical coefficients based on wind tunnel and towing tank model experiments. The rudder model is based on captive manoeuvring experiments to determine the rudder lift and drag and the interactions with hull and propulsion.

## 3.3 Control and Automation

### 3.3.1 Power Management System (PMS)

The power management system (PMS) was designed to control the two gensets depending on the operational mode selected by the user. In the following subsections the operational modes and the control algorithm are described.

#### 3.3.1.1 Operational Mode

The following operational modes were defined for the dynamic model:

- **MANUAL** = The user can select manually the number of gensets to activate or deactivate.



- **AUTO** = The number of gensets to be activated or deactivated is automatically chosen by the control system on the basis of the implemented algorithm

### 3.3.1.2 Control Calculation Chain

As shown in Figure 3-14, the control strategy has been divided into two areas:

- **DROOP LINES** block which set the ICEs droop lines depending the number of Gen-Sets currently synchronized (GenSets Status) with the grid.
- **POWER BALANCE CALCULATOR** block which knowing the:
  - number of GenSets currently synchronized (GenSets Status) with the grid.
  - current electric power consumed by the propulsion motors (Propulsion Power)
  - Electric Power, sum of the Auxiliary, Payload and Hotel ones
  - Electric Propulsion Power requested by the user (Requested Propulsion Power – see §2.6.2).

calculates the power available for propulsion (see §3.3.2) and defines, in case of AUTO mode, the number of GenSets to switch ON. Their activation/deactivation procedure doesn't start immediately when a new power request exceeds or falls within the settled threshold (e.g. GenSet maximum power). The algorithm verifies that the difference with the threshold is greater than a settled limit (10 kW) and that the request stays active for a certain(settable) amount of time (4 s).



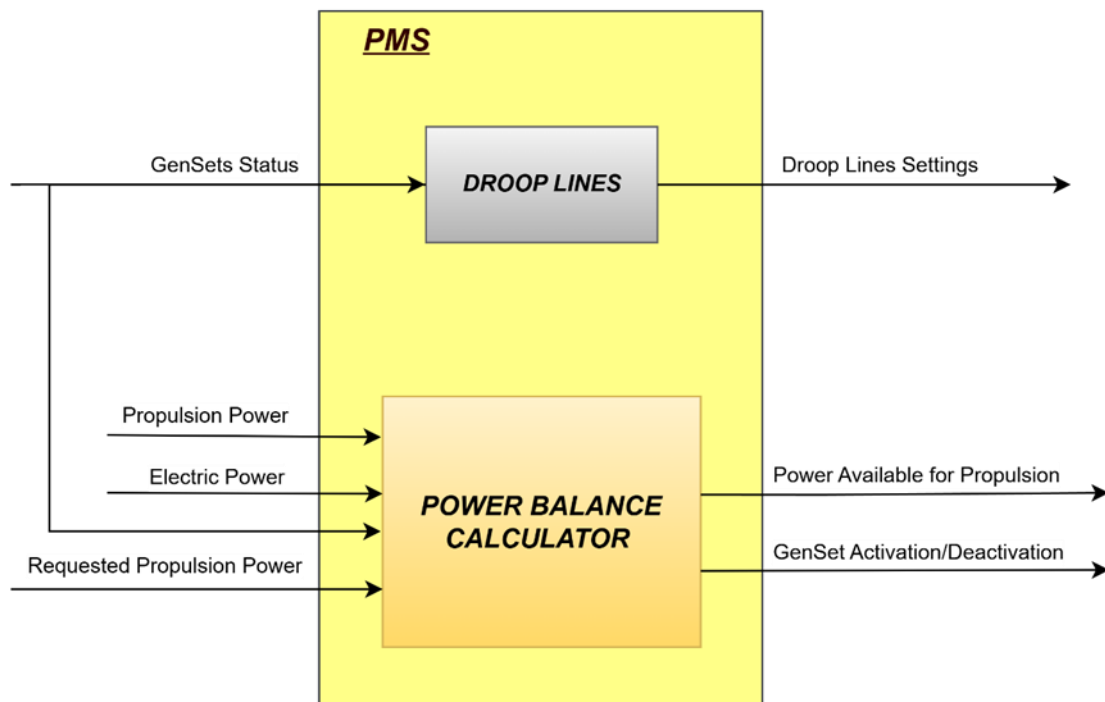


Figure 3-14: PMS Control Strategy Diagram.

### 3.3.2 Propulsion Management System

The propulsion motors are controlled in torque control using the following signals:

- **Current shaft rotational speed.** From this signal it is possible to know the maximum torque and power that the propulsion motors can deliver.
- **Telegraph signal.** This signal expresses the torque set point as a percentage of the maximum torque deliverable by the electric motor. This signal is also used to calculate the mechanical propulsion power request.
- **Mechanical power available for propulsion.** This signal, coming from the PMS, limits the maximum power that the propulsion motors can harvest from the grid in case its value is lesser than the propulsion power request. As consequence, the torque set point will not be directly correlated to the telegraph position but it will be expressed as function of the power available for propulsion. The torque value calculated is used as torque set point for the electric machine.

Figure 3-15 illustrates some of the parameters used for the propulsion management system. It is important to highlight that to make compatible the signal exchange between the PMS and the propulsion management system, the power signals have been converted, depending the conversion direction (electrical to mechanical, or vice versa), with the use of efficiency conversion coefficients. Calculations related to the PMS system concern electrical power whereas the ones made in the propulsion management system are related to mechanical power.



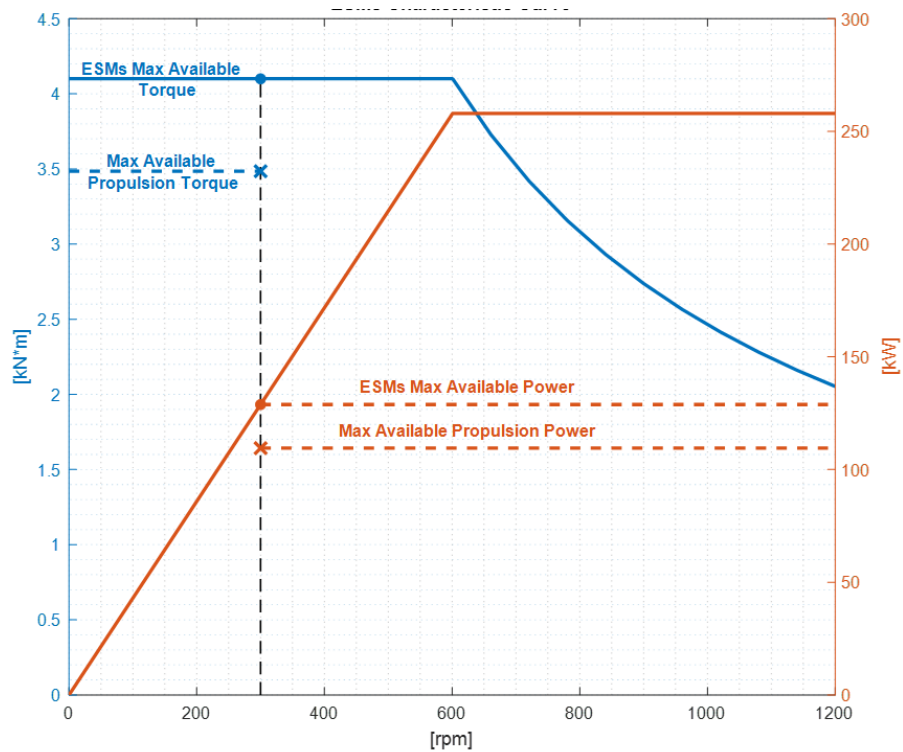


Figure 3-15: Characteristic curves (blue = torque; orange = power) of the electric motors used for propulsion, indicating some parameters used for the propulsion management system.



## 4. Results of verification tests

### 4.1 Results of quasi-static test cases

Using the power time charts from the displayed in Figure 2-1 as input and the quasi-static model described in section 3.1, the fuel consumption and CO<sub>2</sub> equivalent emissions were calculated for the current (diesel direct) and the new design (methanol-electric) of the push boat.

Figure 4-1 shows a comparison between the cumulative fuel consumption of the reference (running on diesel) and the new design. From the graphs a significant difference in fuel consumption is observed. It must be noted that this large difference is mostly due to the difference in energy content between diesel and methanol. As methanol and HVO diesel have a very similar density, the difference in density has little impact in the volume of fuel. However, since the energy content of methanol is approximately the half of that of the diesel, the fuel consumption is approximately double. This can also be seen in Table 4-1, which shows the total fuel consumed by the ship during the operation 'Maintenance of the Danube' (BIO II), represented by test cases TC-1 and TC-2.

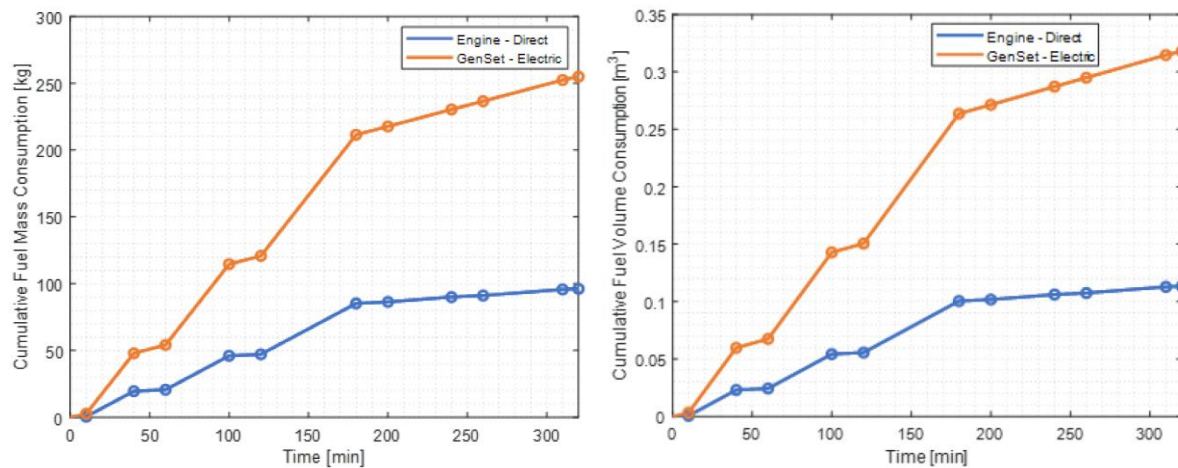


Figure 4-1: Cumulative fuel mass (left) and volume (right) consumed during the operation 'Maintenance of the Danube' (BIO II) for the current (blue) and new (orange) power and energy system architecture of Demo 6.

Table 4-1: Overview of the fuel and energy consumed for the test cases 1 and 2.

Test case	System architecture	Energy carrier	Fuel consumed [kg]	LHV [MJ/kg]	Energy consumed [MJ]
TC-1	Diesel-direct (reference)	Diesel	96.1	42.8	4113.08
		HVO	93.5	44.0	4113.08
TC-2	Methanol-electric (new design)	CH <sub>3</sub> OH (bio-methanol)	254	19.9	5054.6

Using the fuel mass consumption from the quasi-static simulations and the emission factors from Table 3-3 and Table 3-4, the emission values from Figure 4-2 were obtained. These results are displayed graphically in Figure 4-2 and Figure 4-3.



Based on the results of the quasi-static simulations conducted for test case TC-1 and TC-2, it is concluded that the largest reduction in Well-to-Wake CO<sub>2</sub> equivalent emissions is achieved for the new design with methanol-electric propulsion using bio-methanol (i.e., produced from biomass<sup>7</sup>). For this concept, an 84 % reduction in CO<sub>2</sub> emissions is achieved compared to the current design running on diesel. If the current push boat is operated with HVO a reduction of about 67 % in CO<sub>2</sub> Well-to-Wake CO<sub>2</sub> equivalent emissions can be achieved, compared to the current design running on diesel.

For the new design with methanol-electric propulsion using bio-methanol, a very large reduction in NO<sub>x</sub> and particulate matter can be achieved. This reduction is approximately 80 % in NO<sub>x</sub> and 90 % in particulate matter, compared to the current design running on diesel. When the current push boat is operated with HVO, almost a 100 % reduction in NO<sub>x</sub> and particulate matter can be achieved. Despite the large reduction in emissions achieved by using HVO, its limited scalability and availability in the long run may limit the usage of this fuel in the future. For this reason, the use of bio-methanol seems to be a more viable solution, but it should be noted that it also has a limited feedstock.

From the results it can be determined that the usage (and therefore availability for bunkering) of bio-methanol as energy carrier is crucial to achieve the 35 % target in reduction of GHG emissions in inland and coastal shipping.

Table 4-2: Overview of the emissions of the current and new design resulting from the quasi-static test cases TC-1 and TC-2.

Test case	System architecture	Energy carrier	WTW emissions			WTW emissions reduction		
			CO <sub>2</sub> [kg]	NO <sub>x</sub> [kg]	PM [kg]	CO <sub>2</sub> eq [%]	NO <sub>x</sub> [%]	PM [%]
TC-1	Diesel-direct (current design)	Diesel (reference)	179.2	160.8	28.3	0.0	0.0	0.0
		HVO	57.6	0.179	0.014	67.9	99.9	99.9
TC-2	Methanol-electric (new design)	CH <sub>3</sub> OH (bio-methanol)	28.5	28.67	3.45	84	82	88

<sup>7</sup> Biomass from only residual forest wood and straw, as described by pathway #51 in deliverable D1.2 [5].



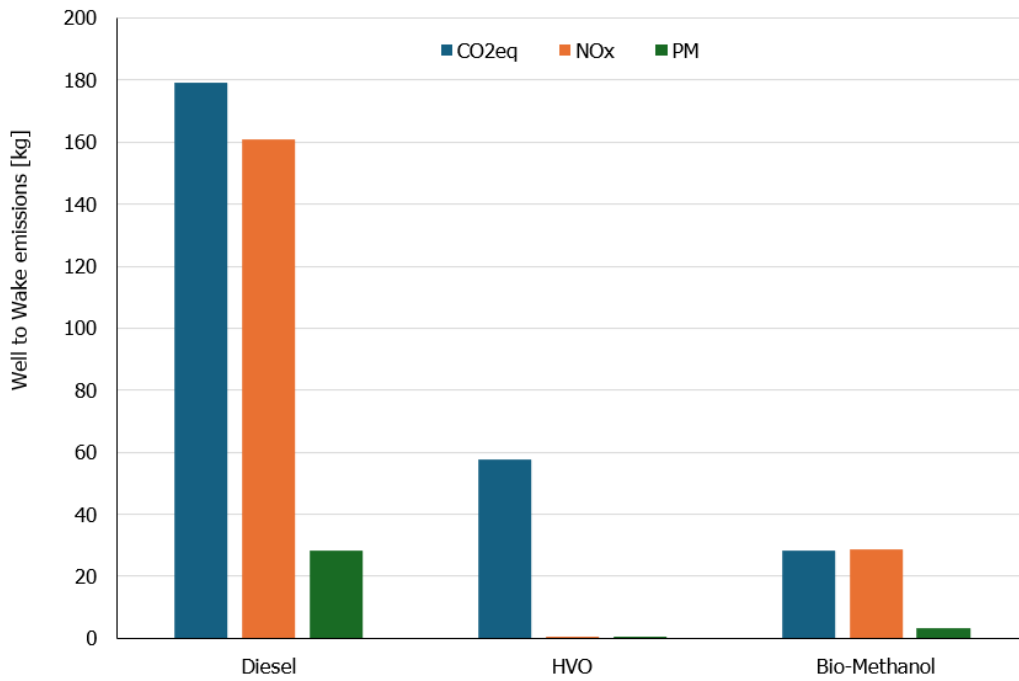


Figure 4-2: Well-to-wake emissions for the current (diesel/HVO) and the new design (bio-Methanol) when performing the operations defined by BIO II.



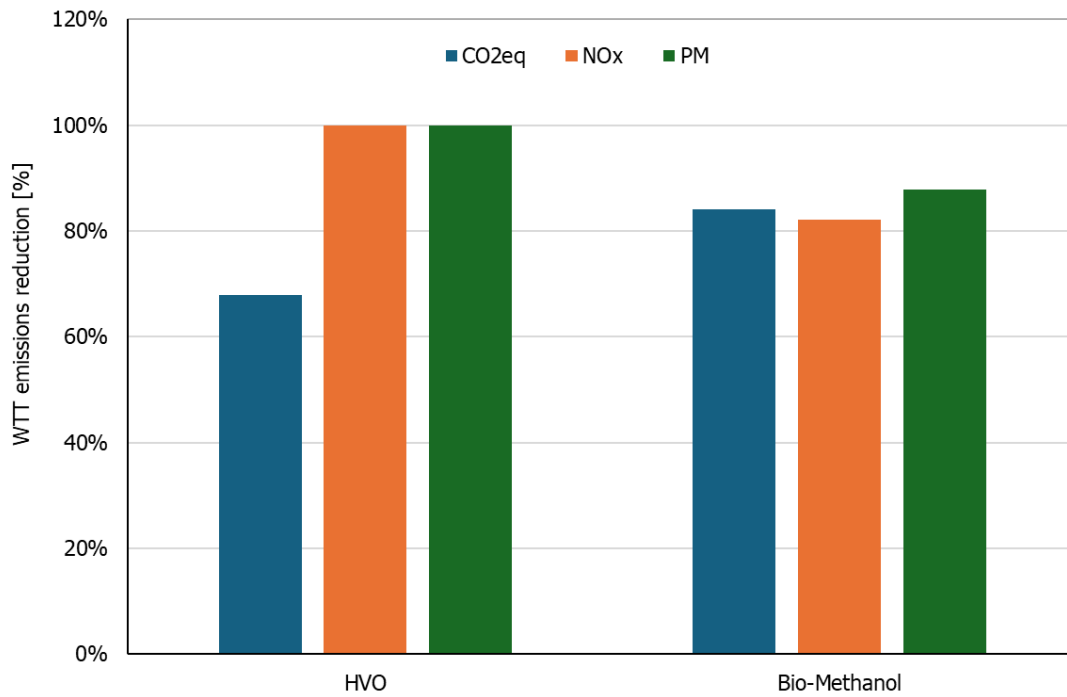


Figure 4-3: Relative reduction in well-to-wake emissions for the current design running with HVO and the new design using bio-Methanol, with respect to the current design running on diesel.



## 4.2 Results of dynamic test cases

### 4.2.1 Test case TC-4: Stopping capacity

The speed of the vessel and distance covered in relation to the ground resulting from the simulation are presented in the graph from Figure 4-4. The results of this test case are summarised in Table 4-3. The simulation was executed under the standard conditions to test the stopping capacity defined by instruction ESI-II-3 in ES-TRIN, therefore the stopping distance in relation to the ground  $s_L$  resulting from the test can be directly compared with maximum allowed stopping distance. As already explained in section 2.3.2.1, for this vessel the stopping distance must be equal or less than 480 m.

Consequently, since  $s_L = 53.4 \text{ m} < 480 \text{ m}$ , it can be concluded that the new design will have sufficient stopping capacity as required by ES-TRIN.

Table 4-3: Main parameters for the stopping capacity of the new barge evaluated in test case TC4.

Main parameter	
Current velocity	$V_{STR} = 1.50 \text{ m/s} \approx 5.4 \text{ km/h}$
Speed of vessel (in relation to the water)	$V_S = 3.61 \text{ m/s} \approx 13 \text{ km/h}$
Speed of vessel (in relation to the ground)	$V_L = 5.11 \text{ m/s} \approx 18.4 \text{ km/h}$
Stopping distance in relation to the water (point A to D)	$S_{MESS\_UNG} = 50 \text{ m}$
Stopping distance in relation to the ground (point A to E)	$S_L = 53.4 \text{ m}$
Loading condition (boat+barge)	$D_{IST} = 146 \text{ m}^3 \approx D_{max}$
Actual draught of convoy	$T_{IST} = 0.8 \text{ m} \approx T_{max}^8$

<sup>8</sup>  $T_{max}$  of barge. Push boat is assuming sailing at  $T_{max}$ , namely 1.1 m draught.



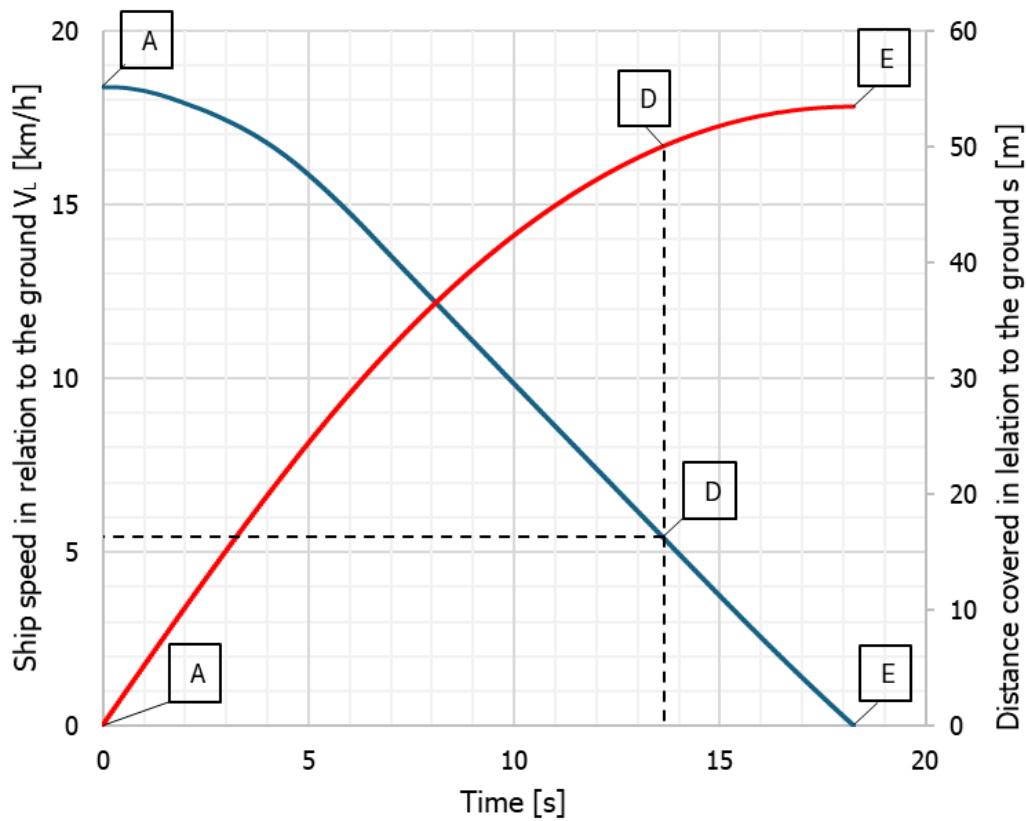


Figure 4-4: Distance covered and speed of vessel in relation to the ground during the stopping manoeuvre simulation performed in test case TC-4. The letters describe the most important points of the manoeuvre as defined in section 2.3.2.1.



#### 4.2.2 Test case TC-5: Capacity for taking evasive action

Following the procedure described in section 2.3.2.2, evasive action manoeuvres were simulated for the new push boat. The simulations were carried out for 20 and 45 degrees rudder angle as required by ES-TRIN. The results of the simulations are collected in Table 4-4 and graphically in Figure 4-5 and Figure 4-6. The test case TC5 for 20 degrees rudder angle can be summarized as follows:

When the ship reaches an equilibrium speed through the water of 13 km/h, the test starts. At this moment,  $t_0 = 0$  is assumed as the initial time. Next, the rudder set point is set to +20 degrees, and then rudder starts turning. Slightly after the rudder has started turning, the vessel begins to turn as well. It can be seen that the turning rate  $r_1$  is achieved before the rudder has reached completely +20 degrees. At this moment time  $t_1$  is recorded. Subsequently, the rudder set point is changed to -20 degrees, which changes the turning direction of the rudder. Despite the rudder angle is being changed to -20 degrees, the turning rate keeps on increasing for some time, resulting in an overshoot in the turning rate. When the overshoot turning rate is reached, the turning rate starts decreasing. When time is  $t_2$ , the turning rate is equal to zero, and subsequently it starts increasing in the opposite direction until the turning rate  $r_3$  is reached, where time  $t_3$  is recorded. After this moment the ruder set point is changed to +20 degrees, causing an overshoot in the turning rate until it becomes zero at the time  $t_4$ , marking the end of the test case.

Test case TC5 for 45 degrees rudder angle display a similar behaviour as the simulation for 20 degrees rudder angle. As expected, the recorded times are slightly higher than for the 45 degrees case.

From the results of the test case it can be seen that the vessel reacts so fast that the rudder does not have time to reach completely the set point. Also, the attained time  $t_4$  for the evasive manoeuvre is well below the limit value, demonstrating that the new design will have sufficient capacity for taking evasive action, satisfying the design requirement by complying with Article 5.09 of ES-TRIN.

Table 4-4: Results of the simulations of evasive action manoeuvres performed for test case TC-5.

Time $t_1$ to $t_4$ required for the evasive action	Rudder angle $\delta$ at which evasive action commences $r_1 = r_3$	
	$\delta = 20$ deg $r_1 = r_3 = 20$ deg/min	$\delta = 45$ deg $r_1 = r_3 = 28$ deg/min
$t_1$ [s]	1.5	1.8
$t_2$ [s]	5.3	6.1
$t_3$ [s]	5.8	6.8
$t_4$ [s]	10.8	12.3
Limit value $t_4$	Limit value $t_4 = 110$ s	



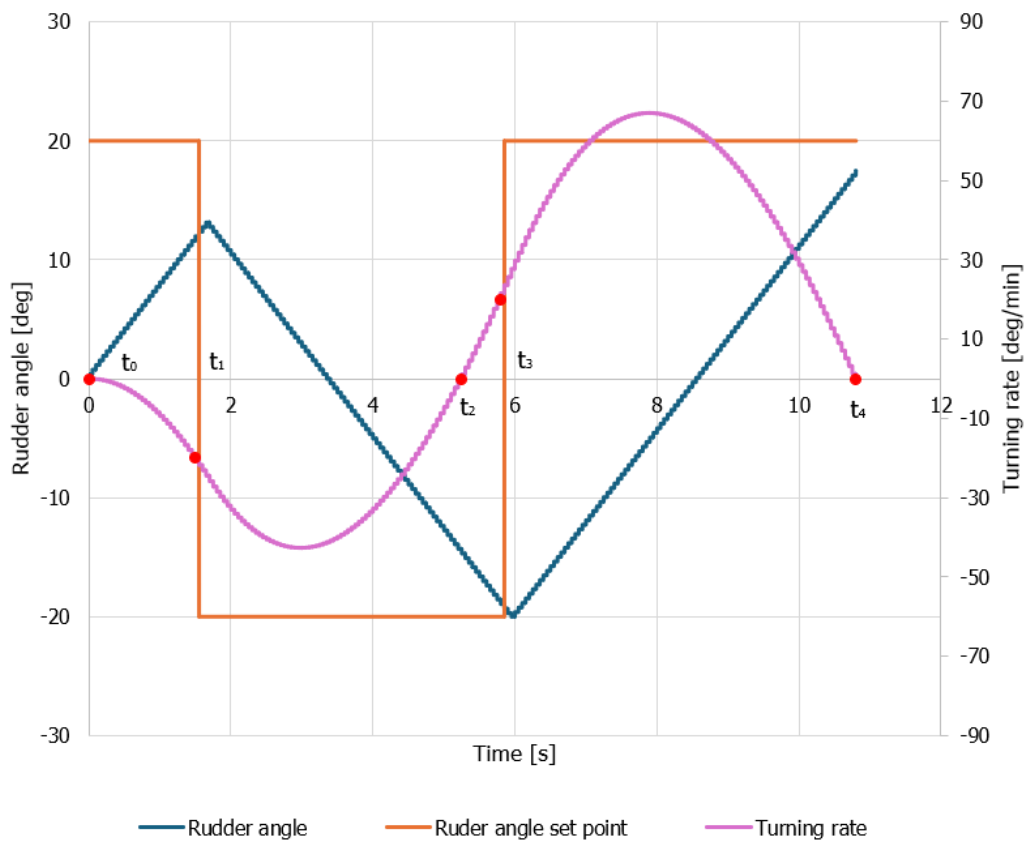


Figure 4-5: Time series of the rudder angle and turning rate resulting from the simulations of test case TC-5 for the evasive manoeuvre at 20 degrees rudder angle.



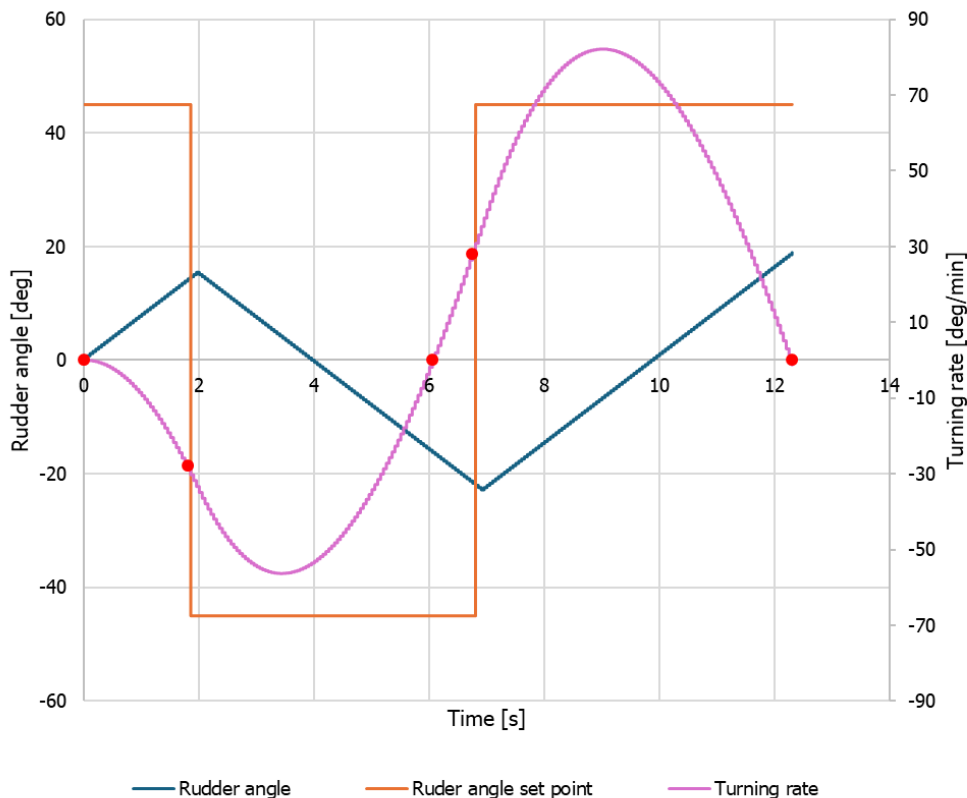


Figure 4-6: Time series of the rudder angle and turning rate resulting from the simulations of test case TC-5 for the evasive manoeuvre at 45 degrees rudder angle.

### 4.2.3 Test case TC-6: Turning capacity

As already mentioned in section 2.3.2.3, ES-TRIN regulations do not include specific requirements to evaluate the turning capacity of the vessel or convoy.

The regulation assumes that if the vessel or convoy satisfies the limit values of the stopping capacity test (test case TC-4), the turning capacity for the vessel/convoy is deemed as sufficient.

In order to evaluate quantitatively the turning capacity of the new design, a dedicated turning circle manoeuvre was carried out sailing upstream at maximum speed. The output parameters from the simulation are presented in Table 4-5, and in Figure 4-7 a top view of the trajectory of the vessel and the main parameters of the turning circle are shown.

Table 4-5: Output parameters from the turning circle manoeuvre conducted for test case TC6.

Parameter	Description	Unit	Value
AD	Advance	m	43.2
		Lpp	1.08
TR	Transfer	m	19
		Lpp	0.48
TD	Tactical diameter	m	56.4
		Lpp	1.41
Dc	Turning diameter	m	56.6
		Lpp	1.42



As no limit values are given in ES-TRIN regulations for the turning circle manoeuvre, the results from Table 4-5 cannot be compared to a reference or limit value. However, if the tactical diameter or the turning diameter are compared to the typical 200 m width of the Austrian Danube, it can be concluded that the convoy (i.e., push boat plus barge) will be able to turn in the river when sailing upstream and at maximum speed, demonstration thus a satisfactory turning capacity.

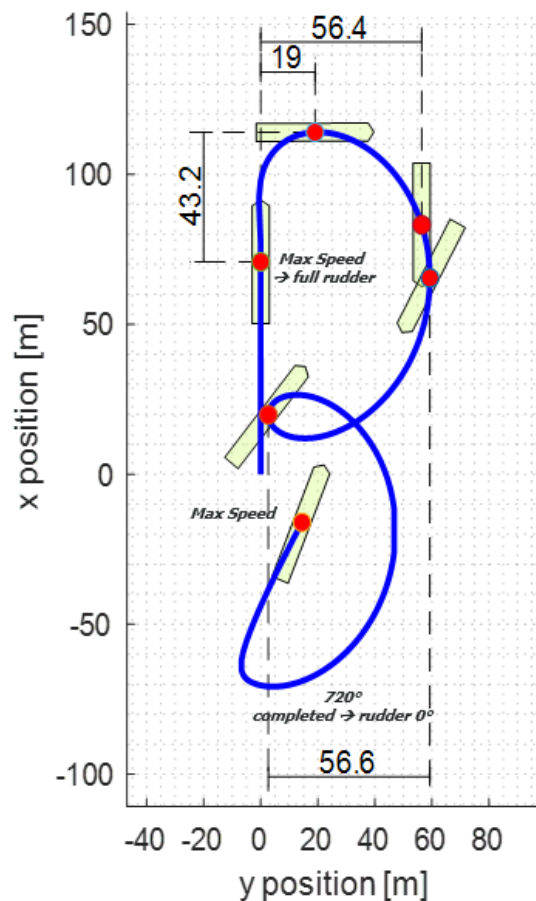


Figure 4-7: Top view showing the trajectory of the ship and barge and the relevant output parameters for test case TC6.



## 5. Conclusions

Based on the results of the simulations of the propulsion and power systems carried out for the reference and new design of the push boat, the following conclusions are derived:

- The largest reduction in Well-to-Wake CO<sub>2</sub> equivalent emissions is achieved for the new design with methanol-electric propulsion using bio-methanol (i.e., produced from biomass<sup>9</sup>). For this concept, an 84 % reduction in CO<sub>2</sub> emissions is achieved compared to the current design running on diesel. If the current push boat is operated with HVO a reduction of about 67 % in Well-to-Wake CO<sub>2</sub> equivalent emissions can be achieved, compared to the current design running on diesel. Despite the large reduction in emissions achieved using HVO, its limited scalability and availability in the long run may limit the usage of this fuel in the future. For this reason, the use of bio-methanol seems to be a more viable solution, but it should be noted that it also has a limited feedstock. Therefore, it can be determined that the usage (and therefore availability for bunkering) of bio-methanol as energy carrier is crucial to achieve the 35 % target in reduction of GHG emissions in inland and coastal shipping.
- For the new design with methanol-electric propulsion using bio-methanol, a very large reduction in NO<sub>x</sub> and particulate matter can be achieved. This reduction is approximately 80 % in NO<sub>x</sub> and 90 % in particulate matter, compared to the current design running on diesel. When the current push boat is operated with HVO, almost a 100 % reduction in NO<sub>x</sub> and particulate matter can be achieved.
- The vessel, sailing with the barge as a single in-line convoy, will be able to stop facing downstream in good time as required by Article 5.07 of ES-TRIN.
- The vessel, sailing with the barge as a single in-line convoy, will be able to take evasive action in good time as required by Article 5.09 of ES-TRIN.
- The vessel, sailing with the barge as a single in-line convoy, will be able to turn in good time since the limit value for stopping facing downstream defined in instruction ESI-II-3 and tested in test case TC4 is not reached. Therefore, the turning capacity requirement specified in Article 5.09 of ES-TRIN will be satisfied. In addition, the vessel sailing with the barge as a single in-line convoy, will be able to turn in a typical free flowing section of Austrian Danube when sailing upstream and at maximum speed, demonstrating thus sufficient turning capacity for its normal operation.

---

<sup>9</sup> Biomass from only residual forest wood and straw, as described by pathway #51 in deliverable D1.2 [5].



## 6. Bibliography

- [1] P. Garcia Barrena and G. Giurco, "SYNERGETICS D3.1 SPEC analyses of full scale and model scale demonstrators," 2024.
- [2] P. Garcia Barrena and G. Giurco, "SYNERGETICS D3.13 Evaluation report viadonau push boat," 2025.
- [3] Central Commission for the Navigation of the Rhine (CCNR), "Mannheim Declaration "150 years of the Mannheim Act – the driving force behind dynamic Rhine and inland navigation"," 17 October 2018. [Online]. Available: [https://www.ccr-zkr.org/files/documents/dmannheim/Mannheimer\\_Erklaerung\\_en.pdf](https://www.ccr-zkr.org/files/documents/dmannheim/Mannheimer_Erklaerung_en.pdf).
- [4] F. Dahlke-Wallat, D. Siebenheller and E. Frank, "SYNERGETICS D4.5 The Catalogue of greening retrofit solutions," 2026.
- [5] F. Thalmann, E. Frank, C. Moser-Stenström and A. Sanchen, "SYNERGETICS D1.2 Report on suitability of identified technical solutions," 2024.
- [6] B. Ramme, "SYNERGETICS D3.17 Evaluation report on application of methanol: compression ignited vs. dual fuel," 2024.
- [7] R. Tonelli and R. Volgels, "Marin rudder mathematical model.," *International Shipbuilding Progress*, 2024.
- [8] International Maritime Organization, Code of safety for ships using gases or other low-flashpoint fuels (IGF Code), 2016.
- [9] International Maritime Organization, International Convention for the Safety of Life at Sea (SOLAS), 1974.
- [10] International Maritime Organization, Technical Code on Control of Emission of Nitrous Oxides from Marine Diesel Engines (NOx Technical Code), 2008.
- [11] H. C. Raven, "A New Correction Procedure for Shallow-Water Effects in Ship Speed Trials," in *PRADS2016*, Copenhagen, 2016.
- [12] I. Bačkalov, "Greening of Inland and Coastal Ships in Europe by Means of Retrofitting: State of the Art and Scenarios," *Sustainability*, vol. 17, no. 11, p. 5154, Jun 2025.
- [13] J. Schweighofer and A. Suvačarov, "Evaluation of the fuel-consumption-reduction potential of a Danube vessel.," in *Transport Research Arena (TRA)*, Vienna, 2018.
- [14] Tonelli, R., "ARD2024: REFS135 manoeuvring mathematical model," MARIN, Wageningen, 2024.
- [15] European Committee for drawing up Standards in the field of Inland Navigation (CESNI), European Standard laying down Technical Requirements for Inland Navigation vessels (ES-TRIN), 2025.